APPENDIX A

Fouruer Analysis Computer Programing

A.1 True Fourier Component Measurement Program.

```
DIM I(500), II(500), IRE(500), IOBSD(500), ANG(500)
DIM FTRE(500, 2), FTIM(500, 2), FTRET(500), FTIMT(500)
P = 0
DO
P = P + 1
CLS
INPUT "INPUT FILE NAME :", N$
INPUT "INPUT N = ", N
INPUT "      A = ", A
INPUT "      B = ", B
INPUT "      D1 = ", D1
INPUT "      DA = ", DA
INPUT "      DB = ", DB
INPUT "      DN = ", DN
INPUT "      CENTRE ANGLE = ", DCDAP
INPUT "      D-SPACING    = ", D
```

```
INPUT "       LAMDA = ", LAMDA
OPEN N$ FOR BINARY AS #1
FOR Y = 1 TO N STEP 1
    GET #1, , IOBSD(Y)
NEXT Y
CLOSE
ANGL = D1
FOR Y = 1 TO N STEP 1
    ANG(Y) = ANGL
    ANGL = ANGL + .01
NEXT Y
REM ------------------------------------------------
----------------
SUMX = 0: SUMY = 0: SUMXY = 0: SUMX2 = 0
FOR I = 1 TO A STEP 1
   SUMX = SUMX + (1 / (DCDAP - ANG(I)) ^ 2)
   SUMY = SUMY + IOBSD(I)
   SUMXY = SUMXY + (IOBSD(I) / (DCDAP - ANG(I)) ^ 2)
   SUMX2 = SUMX2 + (1 / (DCDAP - ANG(I)) ^ 4)
NEXT I
AL = ((A * SUMXY) - (SUMX * SUMY)) / ((A * SUMX2) - SUMX ^
2)
IBGA = (SUMY - (AL * SUMX)) / A
```

```
SUMX = 0: SUMY = 0: SUMXY = 0: SUMX2 = 0
FOR I = B TO N STEP 1
    SUMX = SUMX + (1 / (DCDAP - ANG(I)) ^ 2)
    SUMY = SUMY + IOBSD(I)
    SUMXY = SUMXY + (IOBSD(I) / (DCDAP - ANG(I)) ^ 2)
    SUMX2 = SUMX2 + (1 / (DCDAP - ANG(I)) ^ 4)
NEXT I
C = N - B + 1
AH = ((C * SUMXY) - (SUMX * SUMY)) / ((C * SUMX2) - SUMX ^
2)
IBGB = (SUMY - (AH * SUMX)) / C
REM ------------------------------------------------------
-----------------
FOR Y = 1 TO A STEP 1
   II(Y) = AL / (DCDAP - ANG(Y)) ^ 2
NEXT Y
FOR Y = A + 1 TO B - 1 STEP 1
    II(Y) = IOBSD(Y) - (IBGA - ((IBGA - IBGB) * (ANG(Y) -
ANG(A)) / (ANG(B) - ANG(A))))
NEXT Y
FOR Y = B TO N
    II(Y) = AH / (DCDAP - ANG(Y)) ^ 2
NEXT Y
```

```
 REM ------------------------------------------------------------
------------------
 FOR Y = 1 TO N STEP 1
     I(Y) = 2 * II(Y) / 3
 NEXT Y
 REM ------------------------------------------------------------
------------------
 SUM1 = 0
 FOR Y = 1 TO N STEP 1
     SUM1 = SUM1 + (I(Y) * (ANG(Y) - ANG(1)))
 NEXT Y
 SUM2 = 0
 FOR Y = 1 TO N STEP 1
     SUM2 = SUM2 + I(Y)
 NEXT Y
 DCDAC = ANG(1) + (SUM1 / SUM2)
 PRINT "DCDAC = "; DCDAC
 REM ------------------------------------------------------------
------------------
 FACTOR = 2 * 3.141 * COS(.0174532925# * DCDAC / 2) *
.0174532925# * D / LAMDA
 FOR X = 1 TO 500 STEP 1
     SUM3 = 0
```

```
      FOR Y = 1 TO N STEP 1
          SUM3 = SUM3 + (I(Y) * COS((ANG(Y) - DCDAC) *
FACTOR * X))
      NEXT Y
      FTRE(X, P) = SUM3 / SUM2
 NEXT X
 FOR X = 1 TO 500 STEP 1
      SUM4 = 0
      FOR Y = 1 TO N STEP 1
          SUM4 = SUM4 + (I(Y) * SIN((ANG(Y) - DCDAC) *
FACTOR * X))
      NEXT Y
      FTIM(X, P) = SUM4 / SUM2
 NEXT X
 LOOP UNTIL P = 2
 REM ------------------------------------------------
-----------------
 FOR X = 1 TO 500 STEP 1
      FTRET(X) = ((FTRE(X, 1) * FTRE(X, 2)) + (FTIM(X, 1) *
FTIM(X, 2))) / ((FTRE(X, 2) ^ 2) + (FTIM(X, 2) ^ 2))
      FTIMT(X) = ((FTRE(X, 2) * FTIM(X, 1)) - (FTRE(X, 1) *
FTIM(X, 2))) / ((FTRE(X, 2) ^ 2) + (FTIM(X, 2) ^ 2))
 NEXT X
```

```
 REM ------------------------------------------------------------
------------------
 FOR Y = 1 TO N STEP 1
     SUM5 = 0
     FOR X = 1 TO 500 STEP 1
         SUM5 = SUM5 + (FTRET(X) * COS((ANG(Y) - DCDAC) * X
* FACTOR))
     NEXT X
     IRE(Y) = SUM5
     PRINT ANG(Y), IRE(Y)
 NEXT Y
 REM ------------------------------------------------------------
------------------
 INPUT "INPUT FILE NAME TO SAVE TRUE FOURIER DATA : ", A$
 OPEN A$ FOR BINARY AS #1
 FOR Y = 1 TO N STEP 1
     PUT #1, , IRE(Y)
 NEXT Y
 CLOSE
 PRINT
 PRINT "COMPLETE SAVE"
 END
```

A.2 Complete Fourier Analysis of Line Broadening Program.

```
DIM I(500), II(500), IRE(500), IOBSD(500), ANG(500), DL
(100), L(100)
 DIM FTRE(500, 2), FTIM(500, 2), FTRET(500), FTIMT(500)
 P = 0
 DO
 P = P + 1
 CLS
 PRINT "FILE NUMBER "; P
 INPUT "INPUT FILE NAME :", N$
 INPUT "INPUT N = ", N
 INPUT "       A = ", A
 INPUT "       B = ", B
 INPUT "       D1 = ", D1
 INPUT "       DA = ", DA
 INPUT "       DB = ", DB
 INPUT "       CENTRE ANGLE = ", DCDAP
 LAMDA = 1.54056
 D = LAMDA / (2 * SIN(DCDAP * .0174532925# / 2))
 PRINT "d-spacing = "; D
 OPEN N$ FOR BINARY AS #1
 FOR Y = 1 TO N STEP 1
```

```
    GET #1, , IOBSD(Y)
NEXT Y
CLOSE
ANGL = D1
FOR Y = 1 TO N STEP 1
    ANG(Y) = ANGL
    ANGL = ANGL + .01
    PRINT ANG(Y)
NEXT Y
REM ------------------------------------------------
----------------
SUMX = 0: SUMY = 0: SUMXY = 0: SUMX2 = 0
FOR I = 1 TO A STEP 1
   SUMX = SUMX + (1 / (DCDAP - ANG(I)) ^ 2)
   SUMY = SUMY + IOBSD(I)
   SUMXY = SUMXY + (IOBSD(I) / (DCDAP - ANG(I)) ^ 2)
   SUMX2 = SUMX2 + (1 / (DCDAP - ANG(I)) ^ 4)
NEXT I
AL = ((A * SUMXY) - (SUMX * SUMY)) / ((A * SUMX2) - SUMX ^
2)
IBGA = (SUMY - (AL * SUMX)) / A
SUMX = 0: SUMY = 0: SUMXY = 0: SUMX2 = 0
FOR I = B TO N STEP 1
```

```
    SUMX = SUMX + (1 / (DCDAP - ANG(I)) ^ 2)
    SUMY = SUMY + IOBSD(I)
    SUMXY = SUMXY + (IOBSD(I) / (DCDAP - ANG(I)) ^ 2)
    SUMX2 = SUMX2 + (1 / (DCDAP - ANG(I)) ^ 4)
NEXT I
C = N - B + 1
AH = ((C * SUMXY) - (SUMX * SUMY)) / ((C * SUMX2) - SUMX ^
2)
IBGB = (SUMY - (AH * SUMX)) / C
PRINT "IBGA = "; IBGA
PRINT "IBGB = "; IBGB
REM ------------------------------------------------
-----------------
FOR Y = 1 TO N STEP 1
   II(Y) = IOBSD(Y) - (IBGA - ((IBGA - IBGB) * (ANG(Y) -
ANG(A)) / (ANG(B) - ANG(A))))
NEXT Y
REM ------------------------------------------------
-----------------
FOR Y = 1 TO N STEP 1
    I(Y) = 2 * II(Y) / 3
NEXT Y
INPUT "FILE NAME I(Y) : ", D$
```

```
OPEN D$ FOR BINARY AS #1
FOR Y = 1 TO N STEP 1
     PUT #1, , I(Y)
NEXT Y
CLOSE
REM ----------------------------------------------------
------------------
SUM1 = 0
FOR Y = 1 TO N STEP 1
    SUM1 = SUM1 + (I(Y) * (ANG(Y) - ANG(1)))
NEXT Y
SUM2 = 0
FOR Y = 1 TO N STEP 1
    SUM2 = SUM2 + I(Y)
NEXT Y
DCDAC = ANG(1) + (SUM1 / SUM2)
PRINT "DCDAC = "; DCDAC
REM ----------------------------------------------------
------------------
INPUT "INPUT NUMBER OF FOURIER COMPONENT = ", M
FACTOR = 2 * 3.141 * COS(.0174532925# * DCDAC / 2) *
.0174532925# * D / LAMDA
FOR X = 1 TO M STEP 1
```

```
      SUM3 = 0
      FOR Y = 1 TO N STEP 1
          SUM3 = SUM3 + (I(Y) * COS((ANG(Y) - DCDAC) *
FACTOR * X))
      NEXT Y
      FTRE(X, P) = SUM3 / SUM2
 NEXT X
 FOR X = 1 TO M STEP 1
      SUM4 = 0
      FOR Y = 1 TO N STEP 1
          SUM4 = SUM4 + (I(Y) * SIN((ANG(Y) - DCDAC) *
FACTOR * X))
      NEXT Y
      FTIM(X, P) = SUM4 / SUM2
 NEXT X
 LOOP UNTIL P = 2
 REM ------------------------------------------------
-----------------
 FOR X = 1 TO M STEP 1
      FTRET(X) = ((FTRE(X, 1) * FTRE(X, 2)) + (FTIM(X, 1) *
FTIM(X, 2))) / ((FTRE(X, 2) ^ 2) + (FTIM(X, 2) ^ 2))
      FTIMT(X) = ((FTRE(X, 2) * FTIM(X, 1)) - (FTRE(X, 1) *
FTIM(X, 2))) / ((FTRE(X, 2) ^ 2) + (FTIM(X, 2) ^ 2))
```

```
    PRINT FTRET(X), FTIMT(X)
 NEXT X
 INPUT "PRESS ANY KEY TO CONTINUE", L
 REM ------------------------------------------------
------------------
 FOR Y = 1 TO N STEP 1
     SUM5 = 0
     FOR X = 1 TO M STEP 1
         SUM5 = SUM5 + (FTRET(X) * COS((ANG(Y) - DCDAC) * X
* FACTOR))
     NEXT X
     IRE(Y) = SUM5
     PRINT ANG(Y), IRE(Y)
 NEXT Y
 REM ------------------------------------------------
------------------
 INPUT "INPUT FILE NAME TO SAVE INVERSE FOURIER DATA : ",
A$
 OPEN A$ FOR BINARY AS #1
 FOR Y = 1 TO N STEP 1
     PUT #1, , IRE(Y)
 NEXT Y
 CLOSE
```

```
INPUT "INPUT FILE NAME TO SAVE FTRET DATA : ", B$
OPEN B$ FOR BINARY AS #1
FOR Y = 1 TO M STEP 1
    PUT #1, , FTRET(Y)
NEXT Y
CLOSE
INPUT "INPUT FILE NAME TO SAVE FTIMT DATA : ", C$
OPEN C$ FOR BINARY AS #1
FOR Y = 1 TO M STEP 1
    PUT #1, , FTIMT(Y)
NEXT Y
CLOSE
PRINT
PRINT "COMPLETE SAVE"
CLS
PRINT "Particle Size and Strain Measurement": PRINT :
PRINT
DO
INPUT "Input Range for Particle : X1 = "; X1
INPUT "                           X2 = "; X2
SUMX = 0: SUMY = 0: SUMXY = 0: SUMX2 = 0
N1 = X2 - X1 + 1
FOR X = X1 TO X2 STEP 1
```

```
    SUMX = SUMX + X
    SUMY = SUMY + FTRET(X)
    SUMXY = SUMXY + (FTRET(X) * X)
    SUMX2 = SUMX2 + X ^ 2
NEXT X
SL = ((N1 * SUMXY) - (SUMX * SUMY)) / ((N1 * SUMX2) -
(SUMX ^ 2))
PZ = ABS(D / SL)
PRINT
INPUT "Input Range for Strain : X1 = "; X1
INPUT "                         X2 = "; X2
INPUT "Input l = "; L
PI = 22 / 7
FOR X = X1 TO X2 STEP 1
    ZN = SQR(LOG(1 / FTRET(X)) / 2 * PI ^ 2 * L)
    DL(X) = D * ZN
    L(X) = D * X
NEXT X
SUMX = 0: SUMY = 0: SUMXY = 0: SUMX2 = 0
N2 = X2 - X1 + 1
FOR X = X1 TO X2 STEP 1
    SUMX = SUMX + L(X)
    SUMY = SUMY + DL(X)
```

```
    SUMXY = SUMXY + (L(X) * DL(X))
    SUMX2 = SUMX2 + L(X) ^ 2
NEXT X
ST = ((N2 * SUMXY) - (SUMX * SUMY)) / ((N2 * SUMX2) -
(SUMX ^ 2))
PRINT : PRINT : PRINT
PRINT "------------------------------------------------"
PRINT "Average Particle Size = "; PZ; "  Angstrom."
PRINT "Average Strain        = "; ST
PRINT "------------------------------------------------"
PRINT : PRINT : PRINT : INPUT "Measure again? (Y/N) "; G$
LOOP UNTIL G$ = "N"
END
```

A.3 Particle Size and Microstrain Measurement Program.

```
CLS
 DIM DL(500), L(500), FTRET(500)
 INPUT "Input FTRET File Name : "; F$
 INPUT "Number of data = "; N
 OPEN F$ FOR BINARY AS #1
 FOR X = 1 TO N
     GET #1, , FTRET(X)
 NEXT X
 CLOSE
 FOR X = 1 TO N
 PRINT FTRET(X)
 NEXT X
 PRINT "Particle Size and Strain Measurement": PRINT :
PRINT
 DO
 INPUT "Input Range for Particle : X1 = "; X1
 INPUT "                           X2 = "; X2
 INPUT "             d-spacing of peak = "; D
 SUMX = 0: SUMY = 0: SUMXY = 0: SUMX2 = 0
 N1 = X2 - X1 + 1
 FOR X = X1 TO X2 STEP 1
```

```
    SUMX = SUMX + X
    SUMY = SUMY + FTRET(X)
    SUMXY = SUMXY + (FTRET(X) * X)
    SUMX2 = SUMX2 + X ^ 2
NEXT X
SL = ((N1 * SUMXY) - (SUMX * SUMY)) / ((N1 * SUMX2) -
(SUMX ^ 2))
PZ = ABS(D / SL)
PRINT
INPUT "Input Range for Strain : X1 = "; X1
INPUT "                         X2 = "; X2
INPUT "Input l = "; L
PI = 22 / 7
FOR X = X1 TO X2 STEP 1
   ZN = SQR(LOG(1 / FTRET(X)) / 2 * PI ^ 2 * L)
    DL(X) = D * ZN
    L(X) = D * X
NEXT X
INPUT B$
SUMX = 0: SUMY = 0: SUMXY = 0: SUMX2 = 0
N2 = X2 - X1 + 1
FOR X = X1 TO X2 STEP 1
    SUMX = SUMX + L(X)
```

```
        SUMY = SUMY + DL(X)
        SUMXY = SUMXY + (L(X) * DL(X))
        SUMX2 = SUMX2 + L(X) ^ 2
    NEXT X
    PRINT SUMX; SUMY; SUMXY; SUMX2
    ST = ((N2 * SUMXY) - (SUMX * SUMY)) / ((N2 * SUMX2) -
(SUMX ^ 2))
    PRINT : PRINT : PRINT
    PRINT "-------------------------------------------------"
    PRINT "Average Particle Size = "; PZ; "  Angstrom."
    PRINT "Average Strain        = "; ST
    PRINT "-------------------------------------------------"
    PRINT : PRINT : PRINT : INPUT "Measure again? (Y/N) "; G$
    LOOP UNTIL G$ = "N"
    END
```

A.4 Program to Save Data of Line Profile.

```
CLS
 DIM I(500)
 DO
 INPUT "INPUT DATA FILE NAME : ", N$
 INPUT "INPUT NUMBER OF DATA : ", N
 FOR Y = 1 TO N
     PRINT "DATA NO."; Y
     INPUT I(Y)
 NEXT Y
 OPEN N$ FOR BINARY AS #1
 FOR Y = 1 TO N
     PUT #1, , I(Y)
 NEXT Y
 CLOSE
 INPUT "SAVE FOR NEXT PEAK? (Y/N)", A$
 LOOP UNTIL A$ = "N"
 END
```

A.5 Program to Change Data in Data File.

```
CLS
 PRINT "PROGRAM FOR CHANGE DATA IN FILES"
 INPUT "INPUT FILE NAME :", N$
 DO
 INPUT "INPUT LOCAL OF DATA :", R
 INPUT "INPUT NEW DATA :", I
 OPEN N$ FOR BINARY AS #1
    PUT #1, R, I
 CLOSE
 INPUT "MORE DATA ? (Y/N)", A$
 LOOP UNTIL A$ = "N"
 END
```

APPENDIX B

X-Ray Diffraction Pattern of PZT Powder

B.1 Line Profile of PZT Powder Calcined at Temperatures of 400-1300 °C.

400 °C

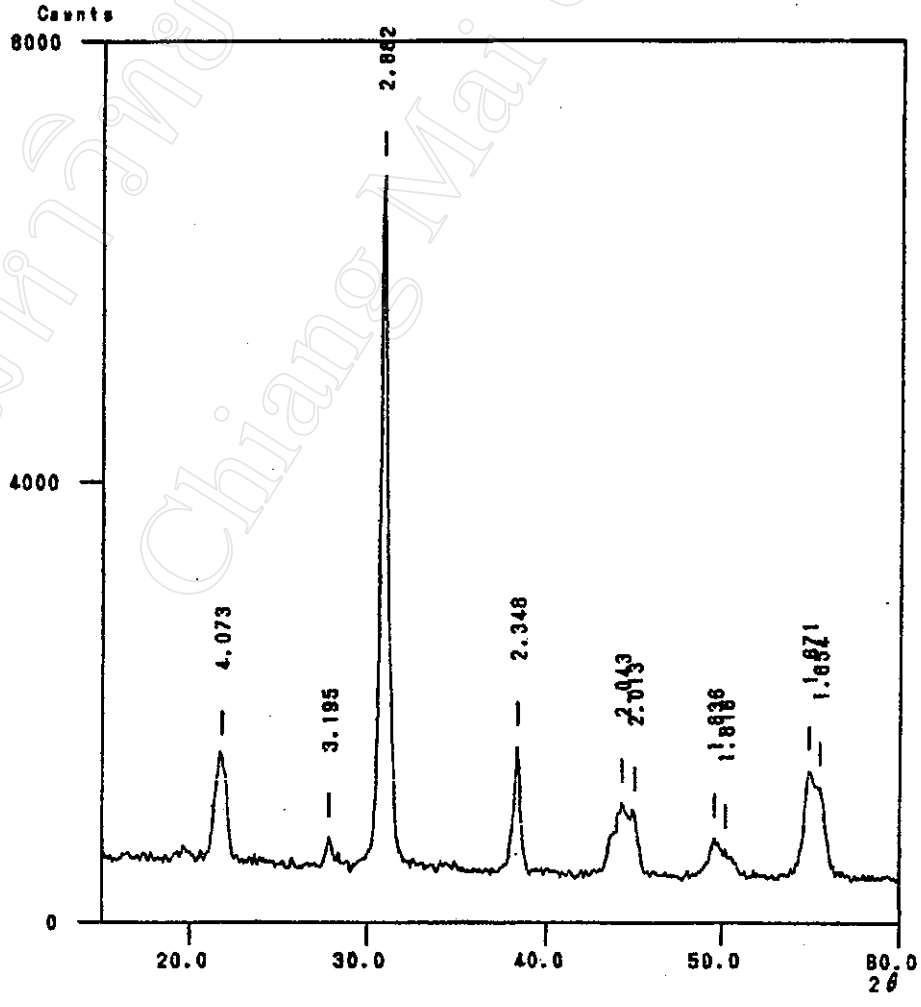

500 °C

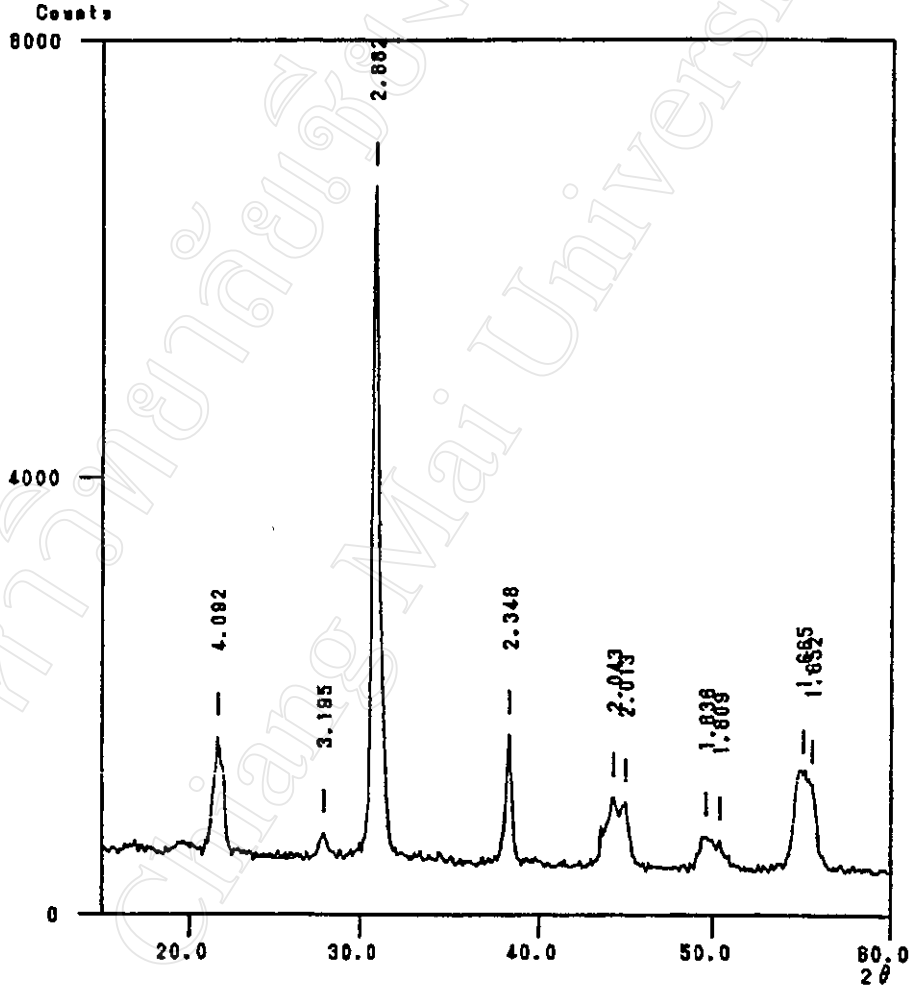

600 °C

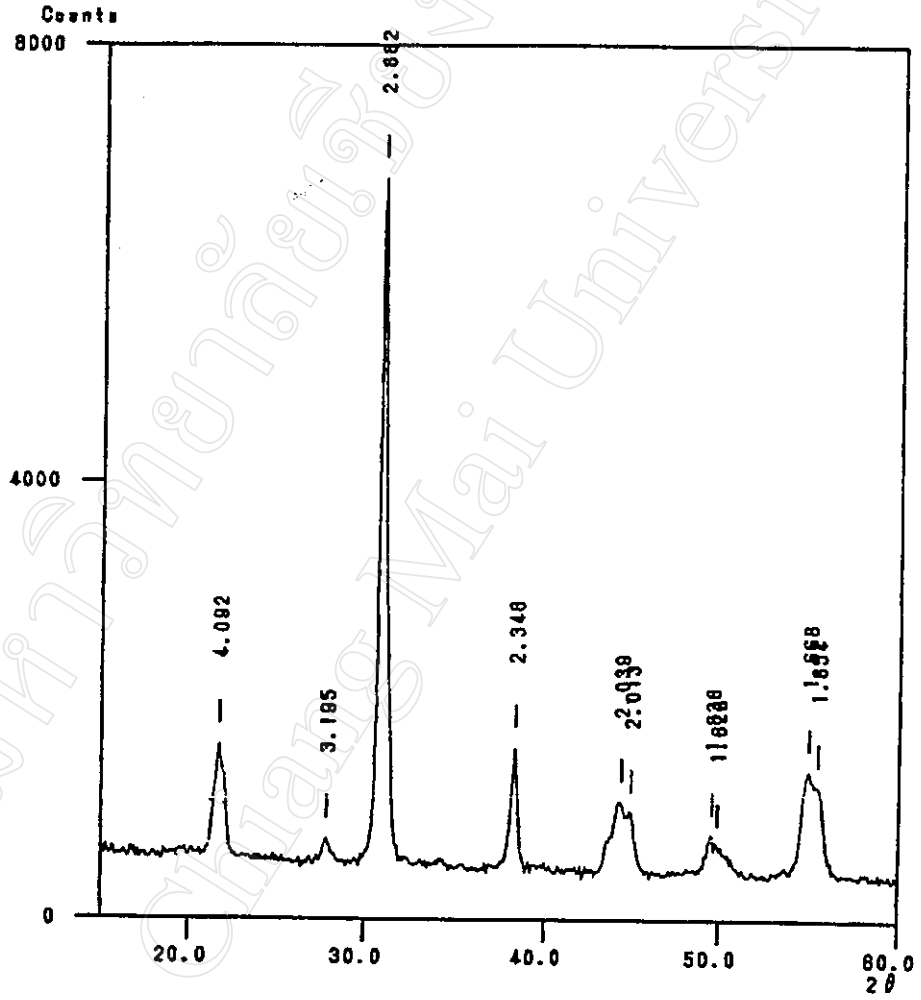

700 °C

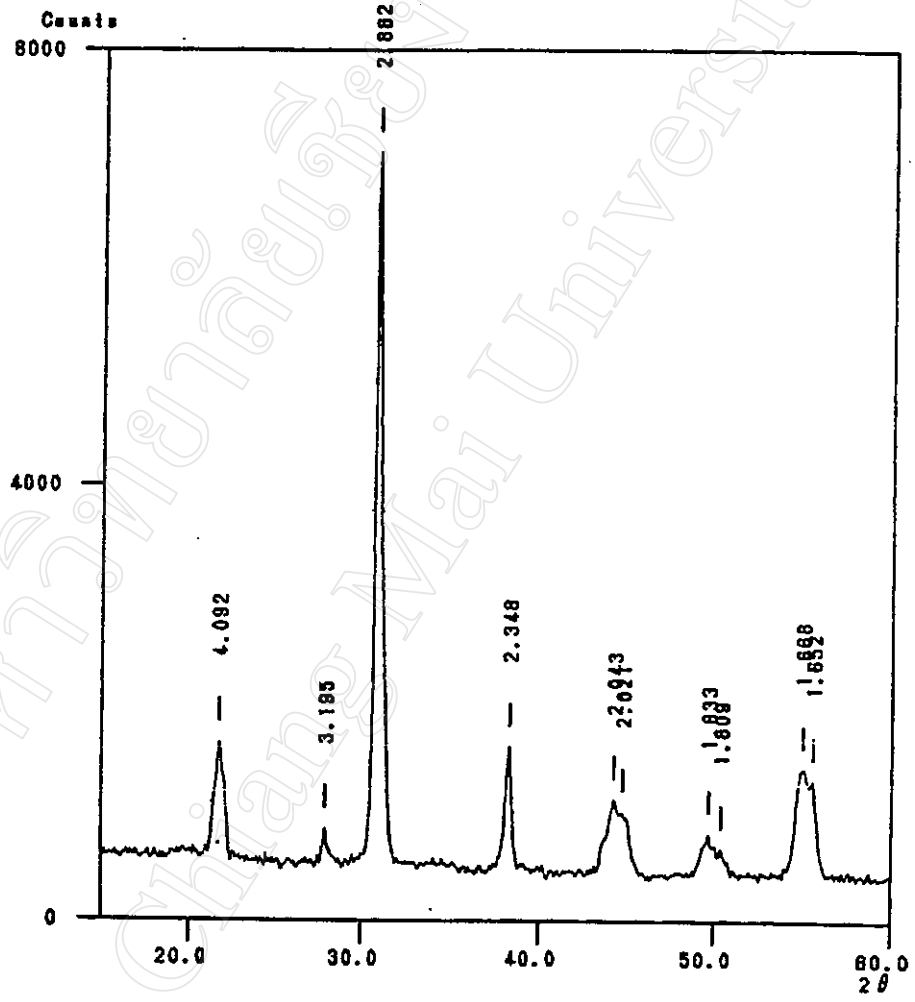

800 °C

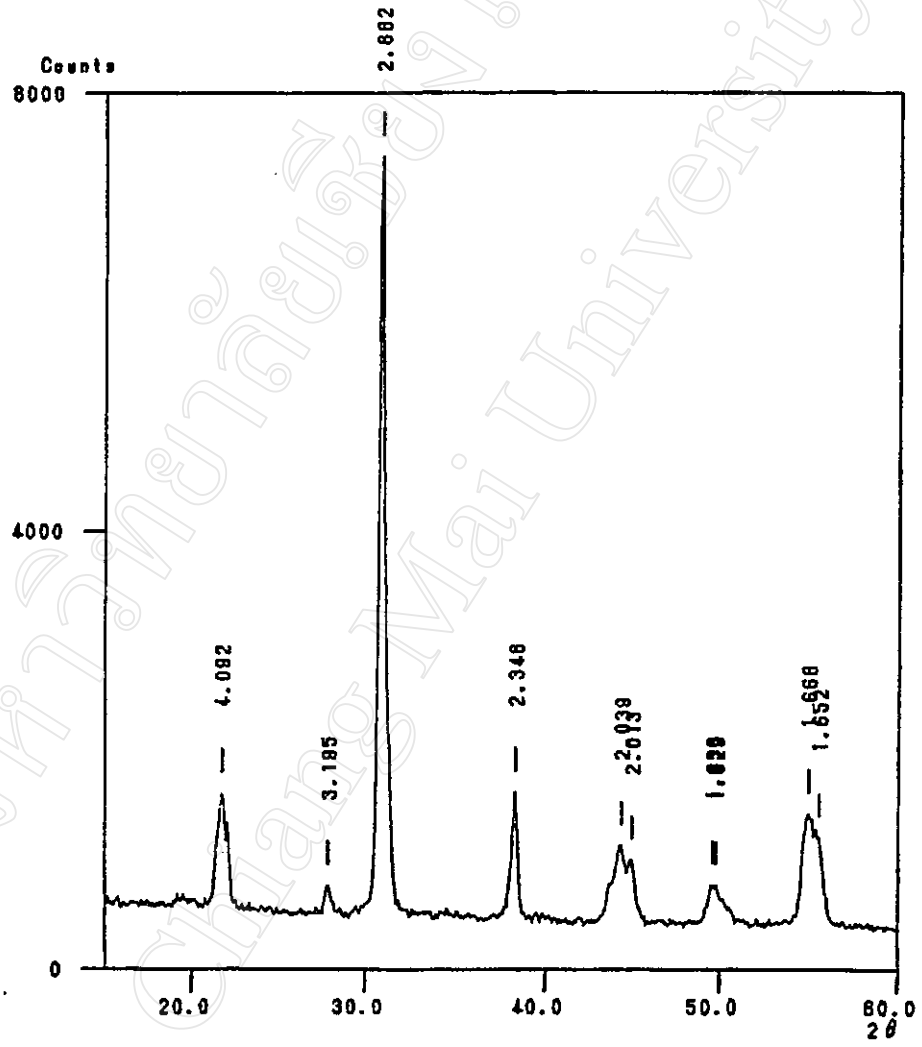

900 °C

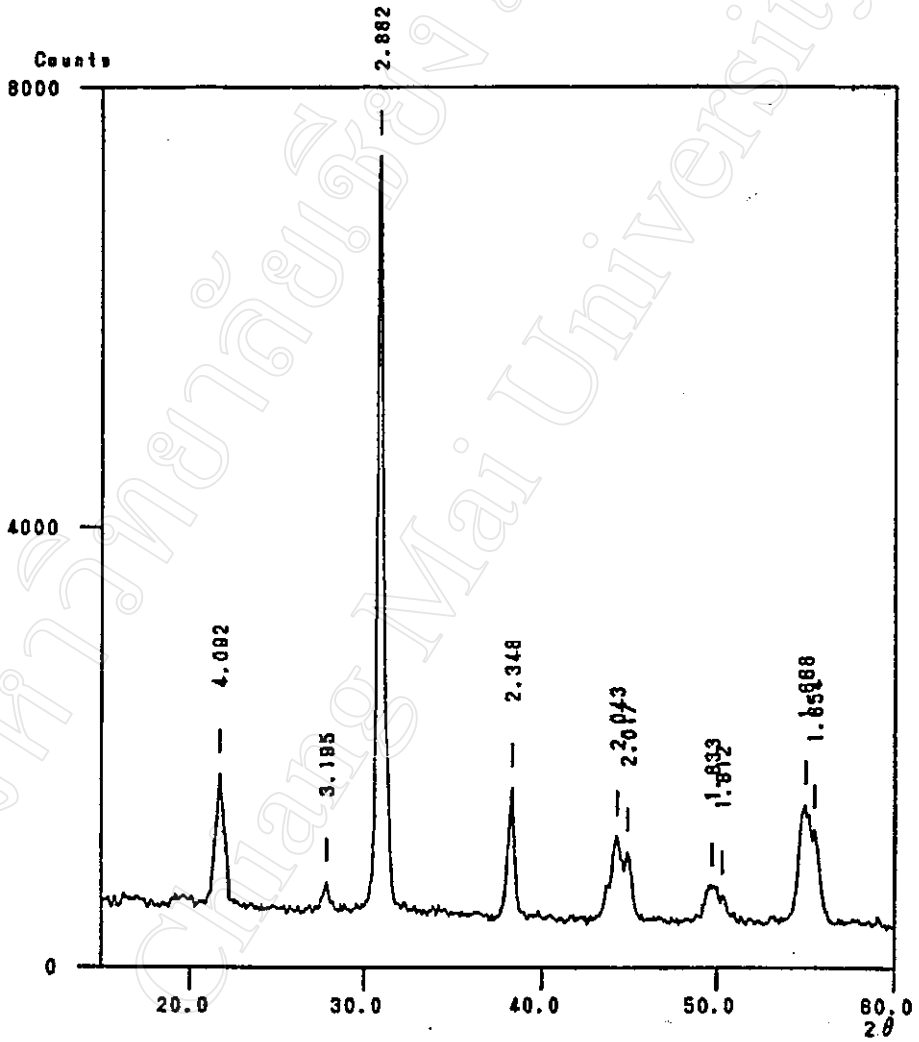

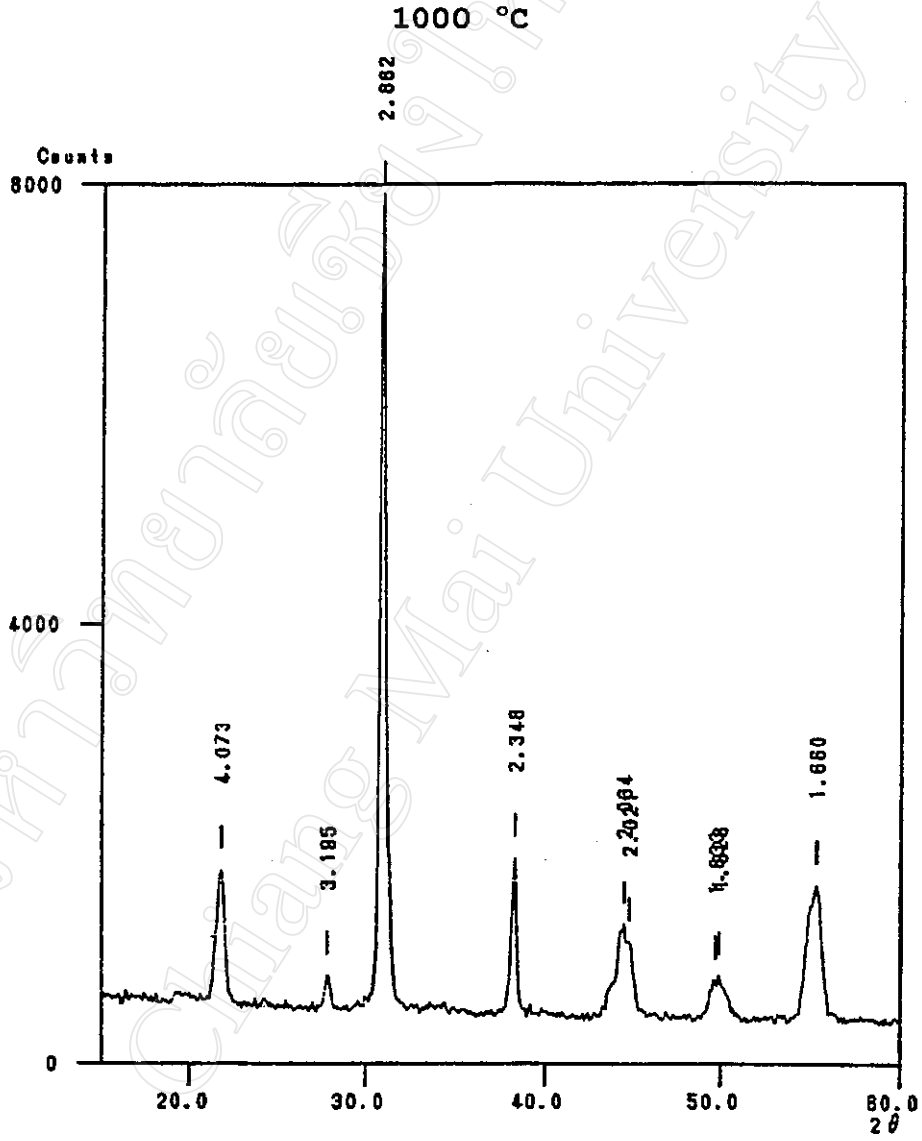

1100 °C

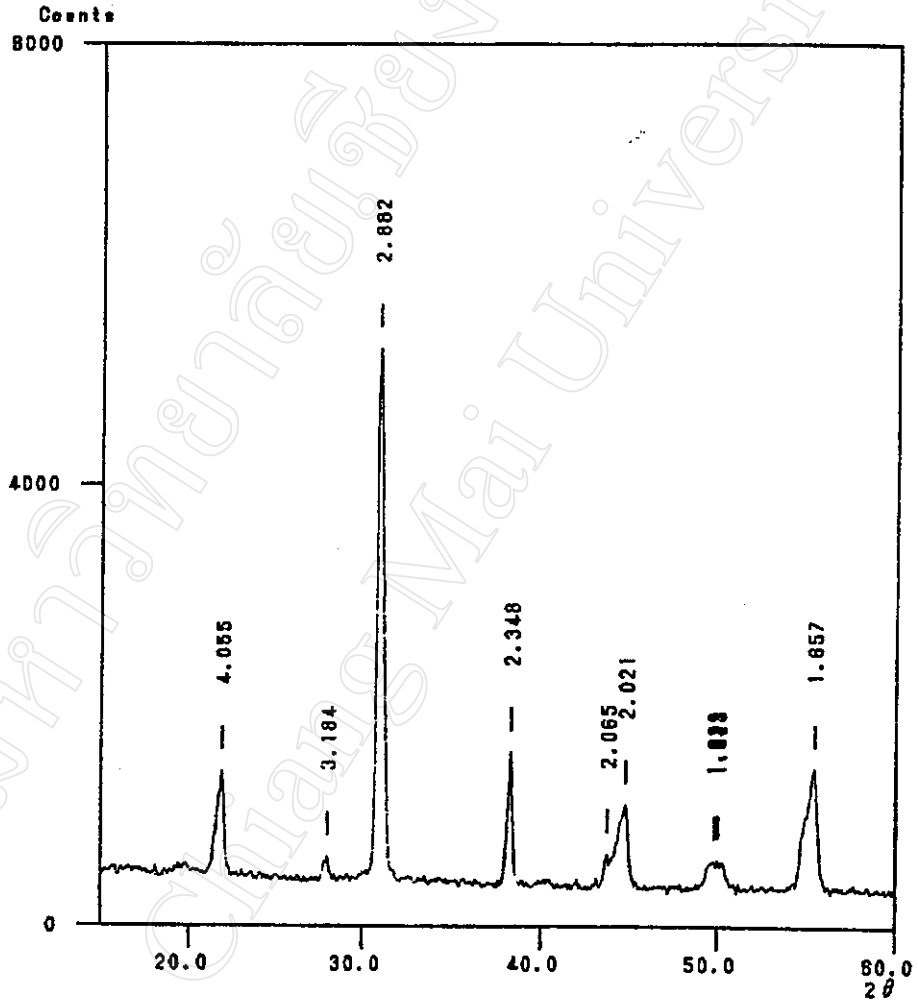

1200 °C

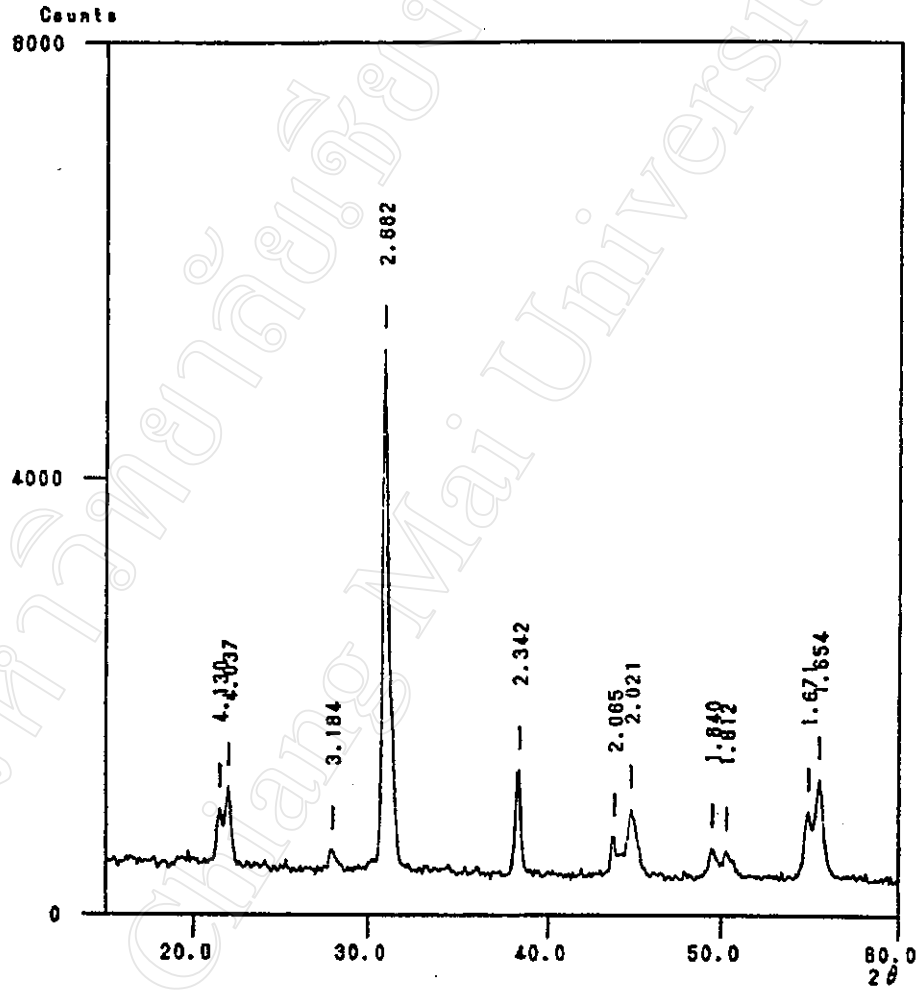

1300 °C

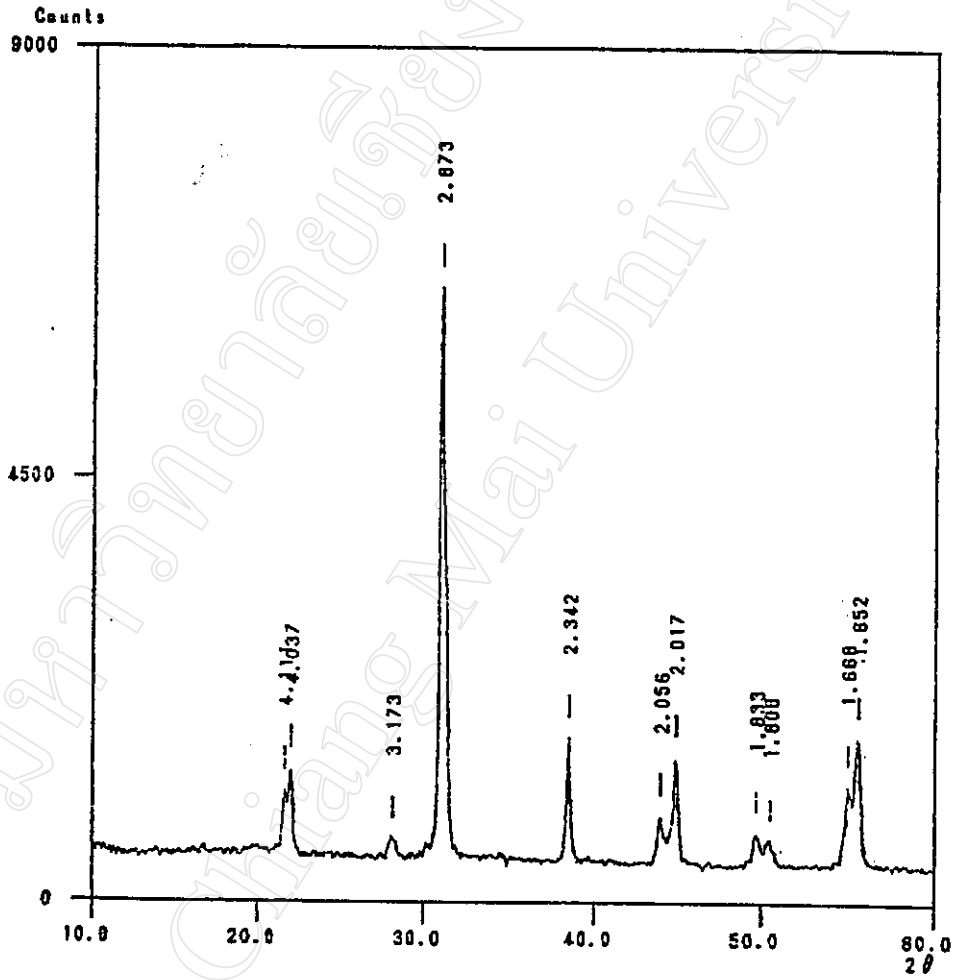

B.2 XRD Line Profile of Peak (111) of PZT Powder Calcined at Temperatures of 400-1300 °C.

400 °C

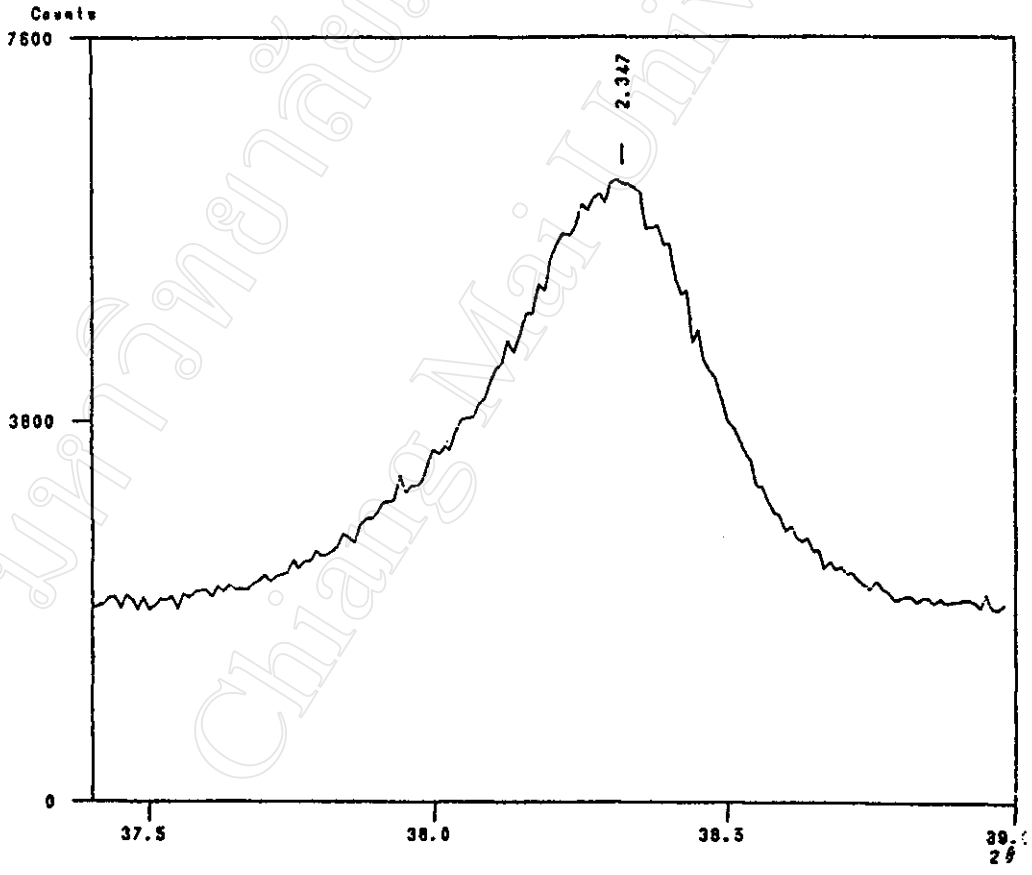

500 °C

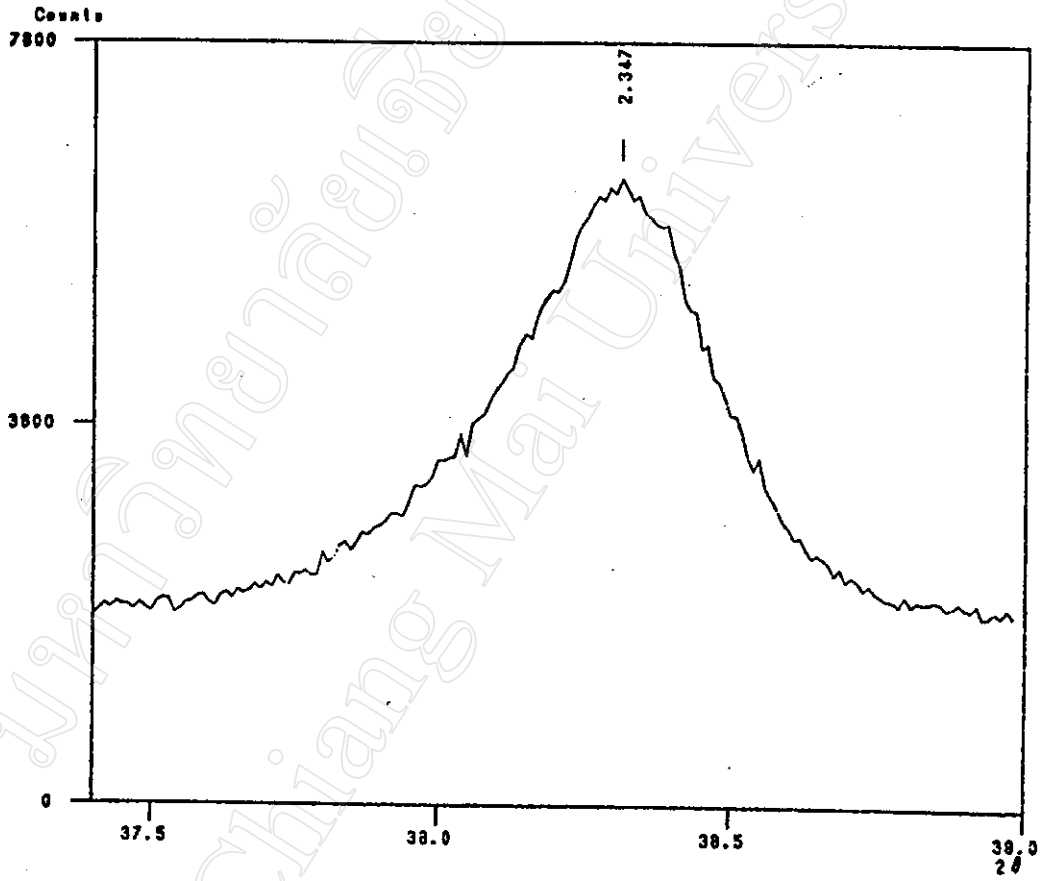

600 °C

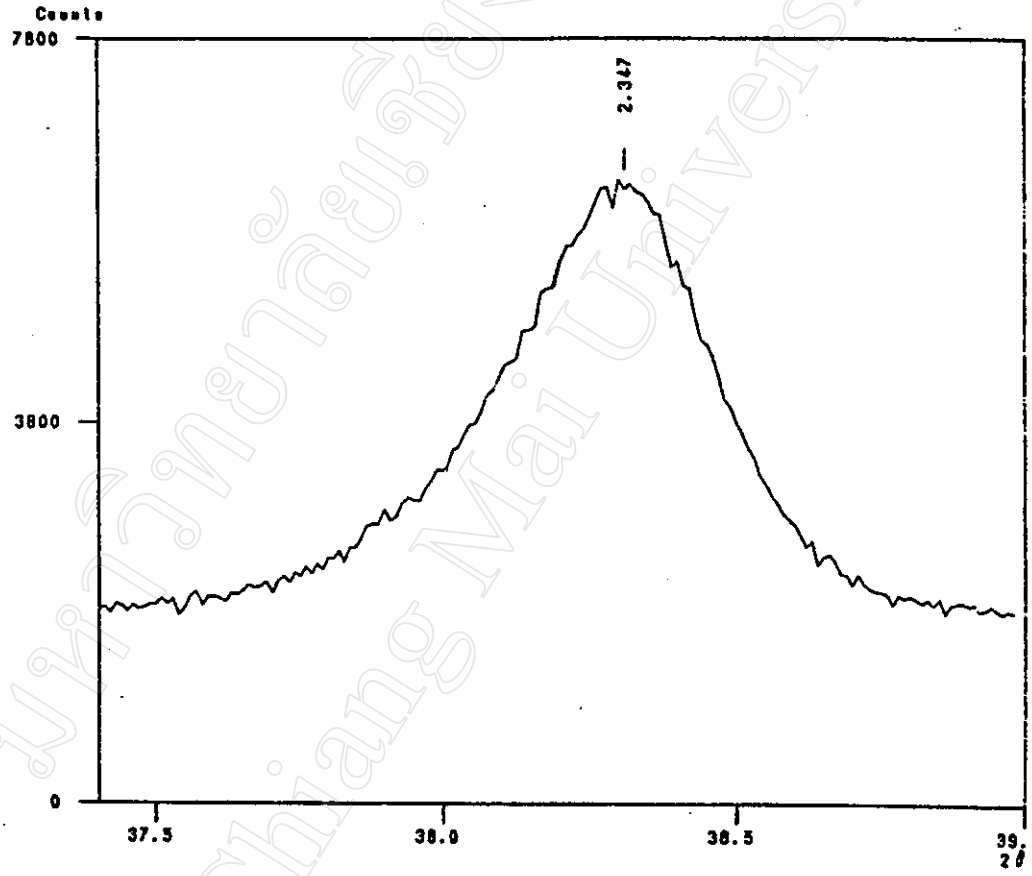

700 °C

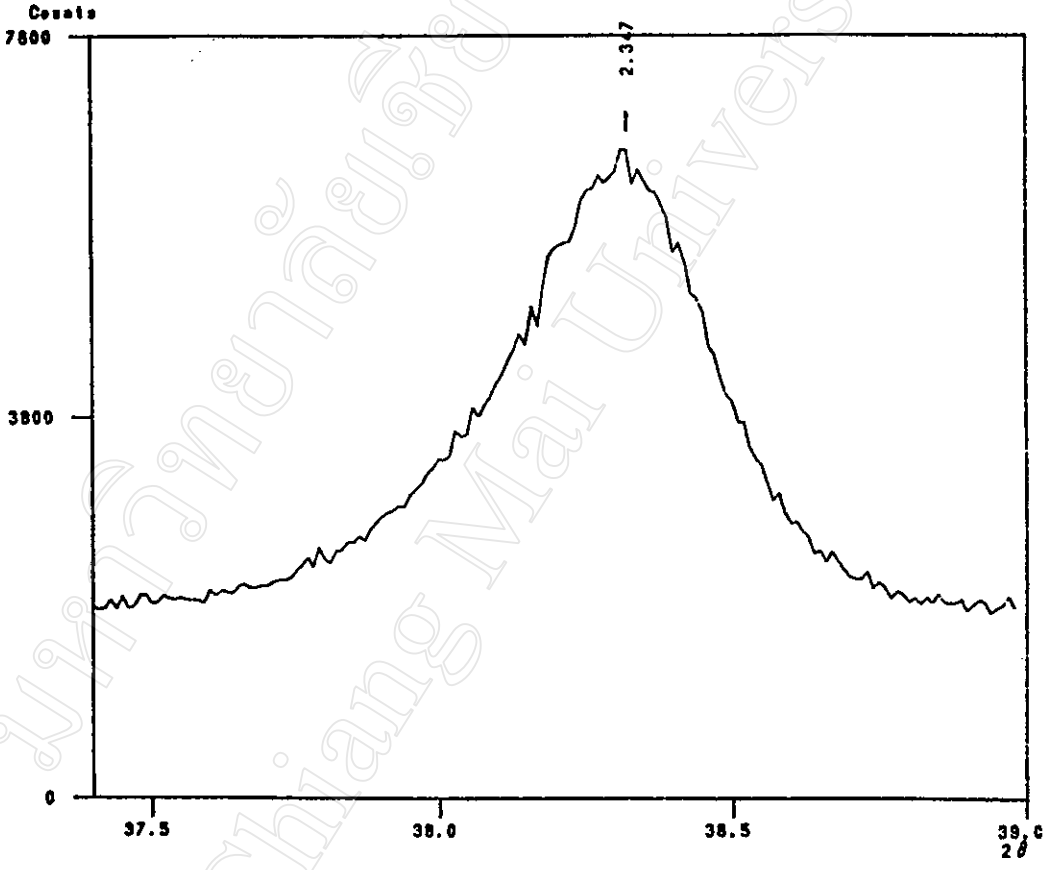

800 °C

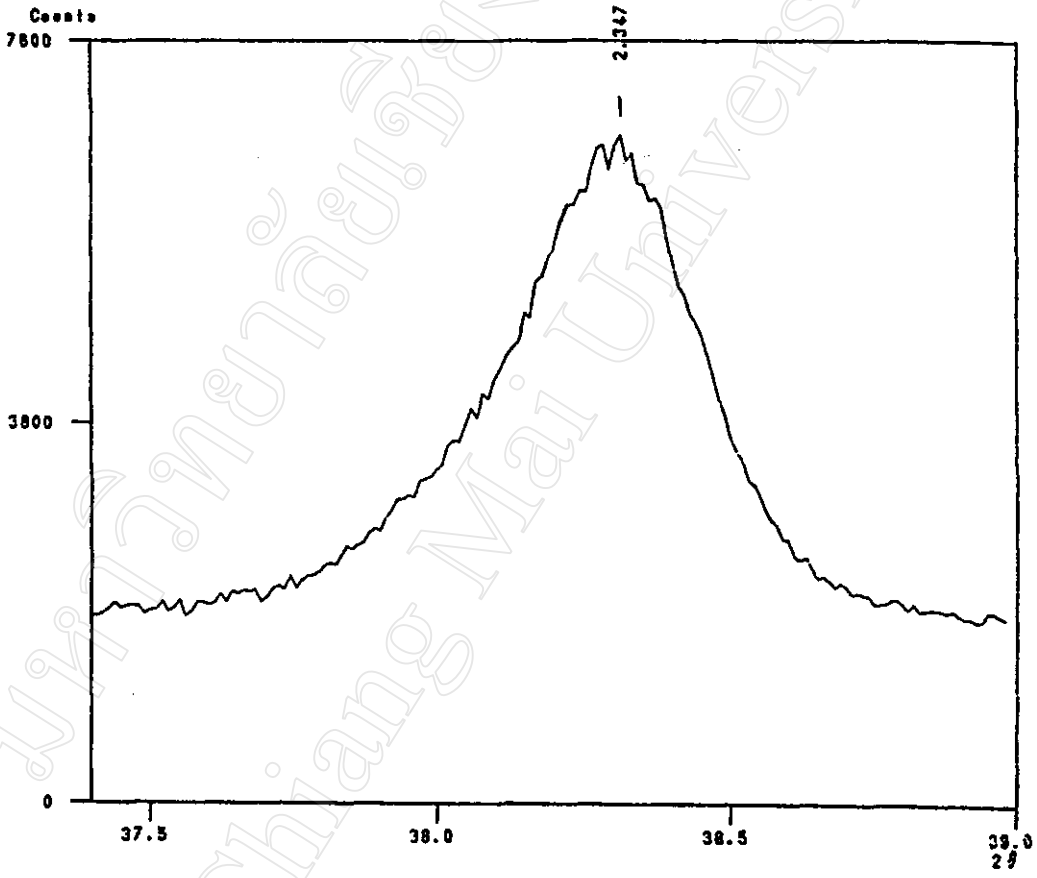

900 °C

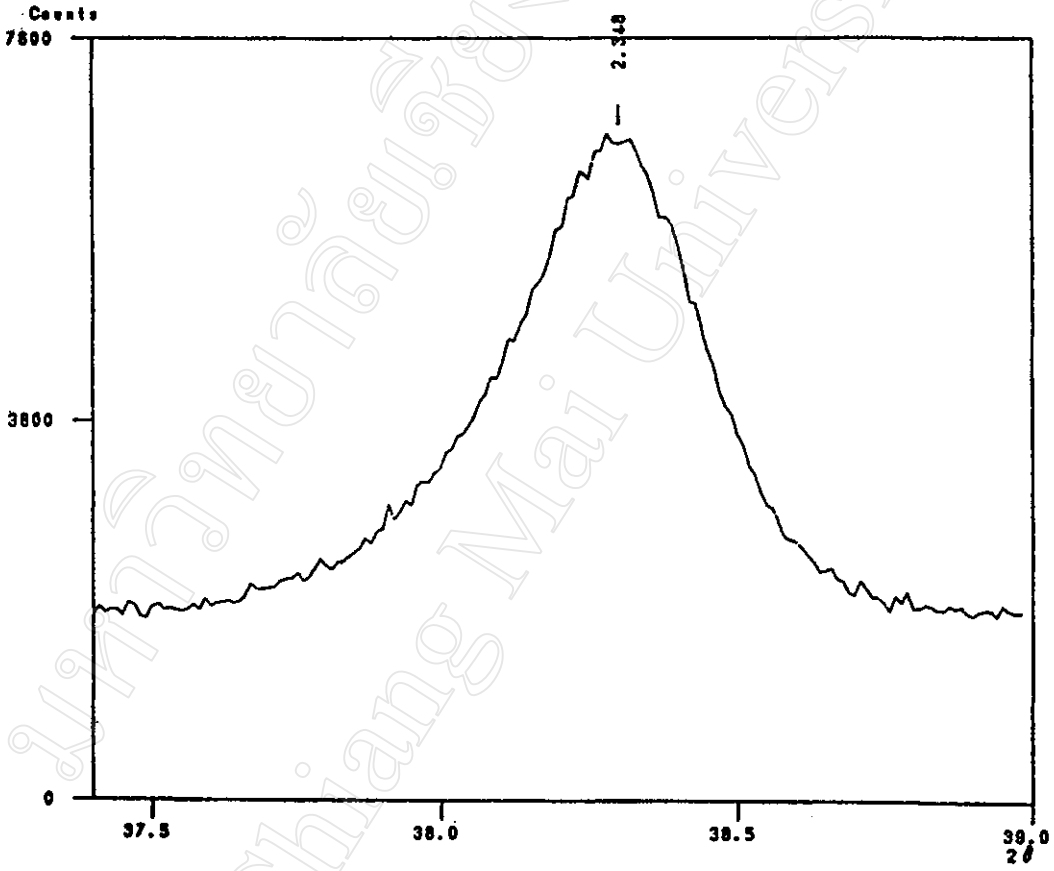

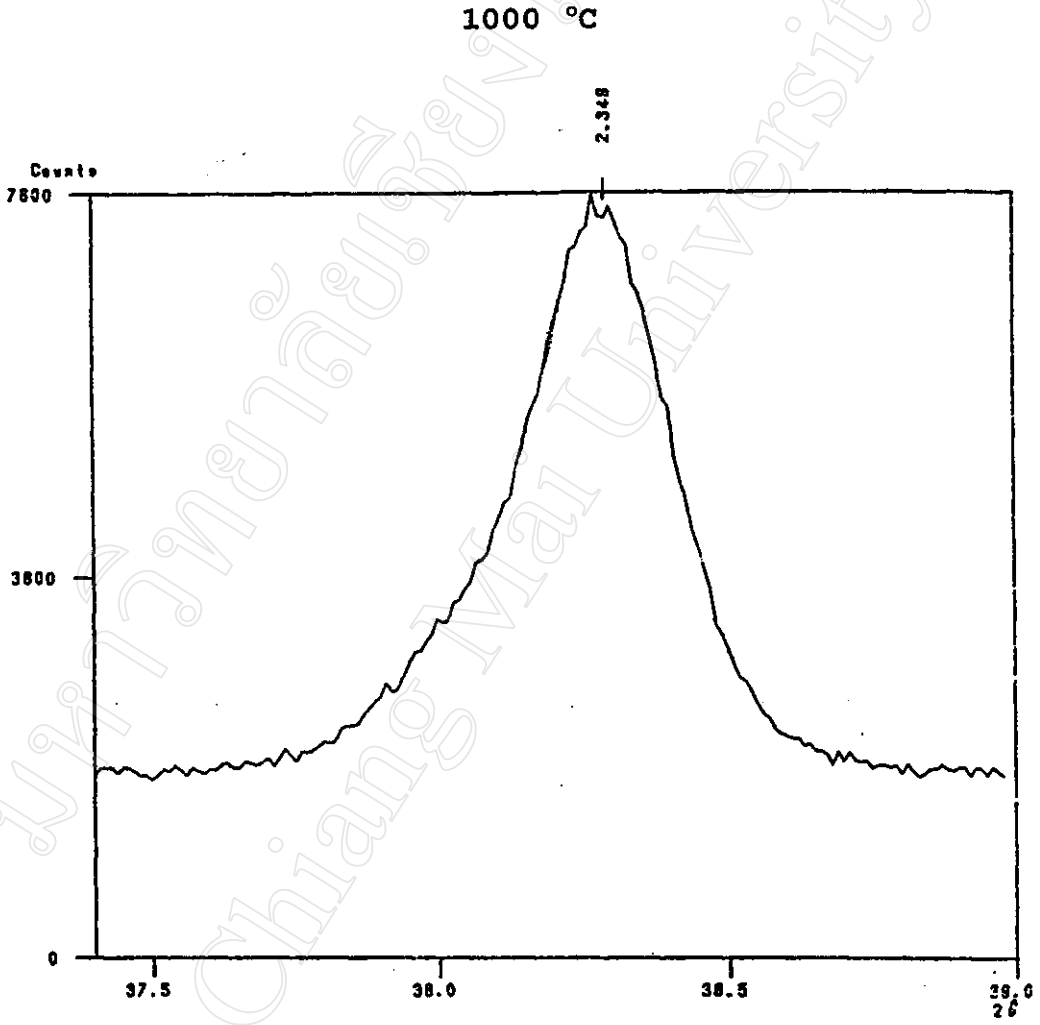

1100 °C

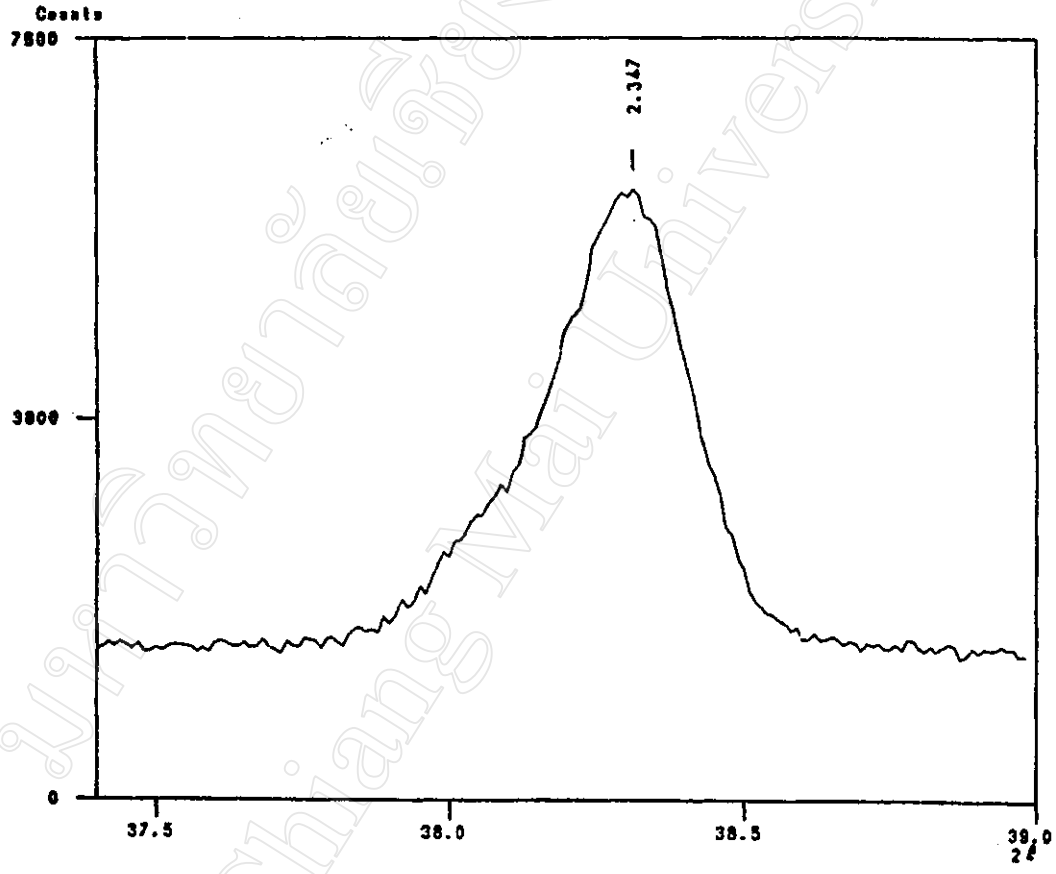

1200 °C

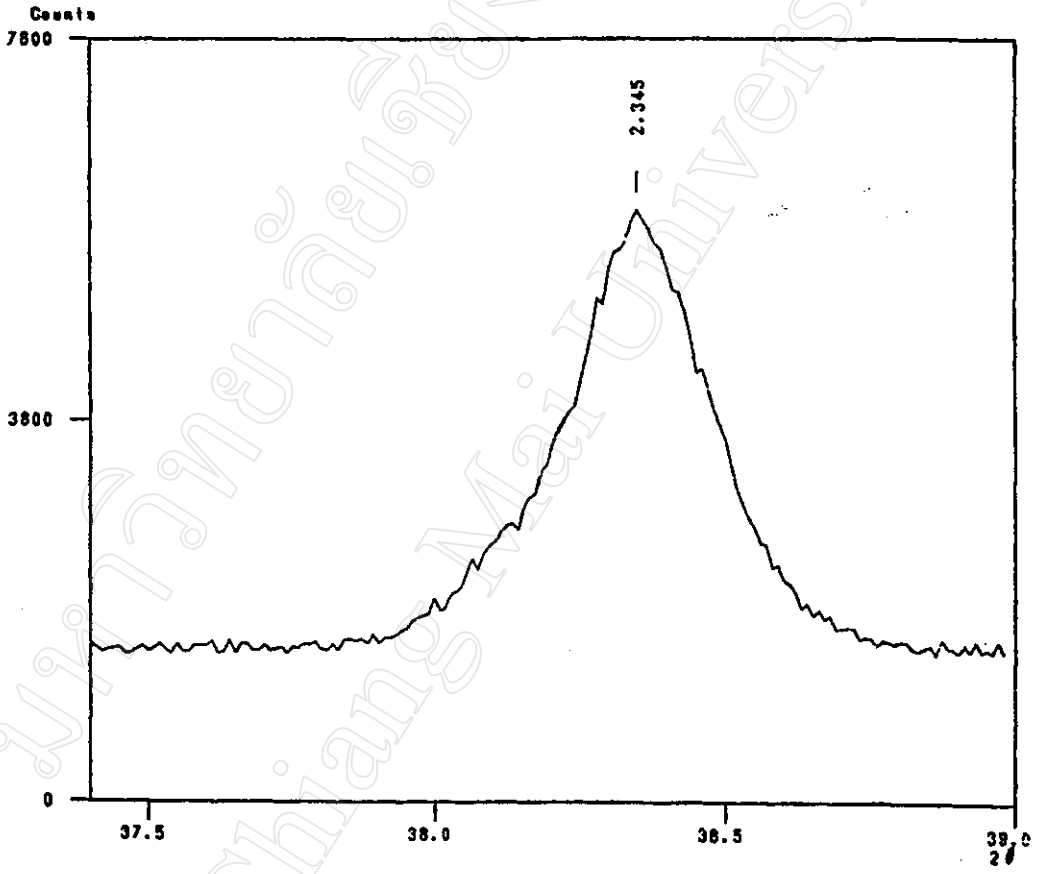

1300 °C

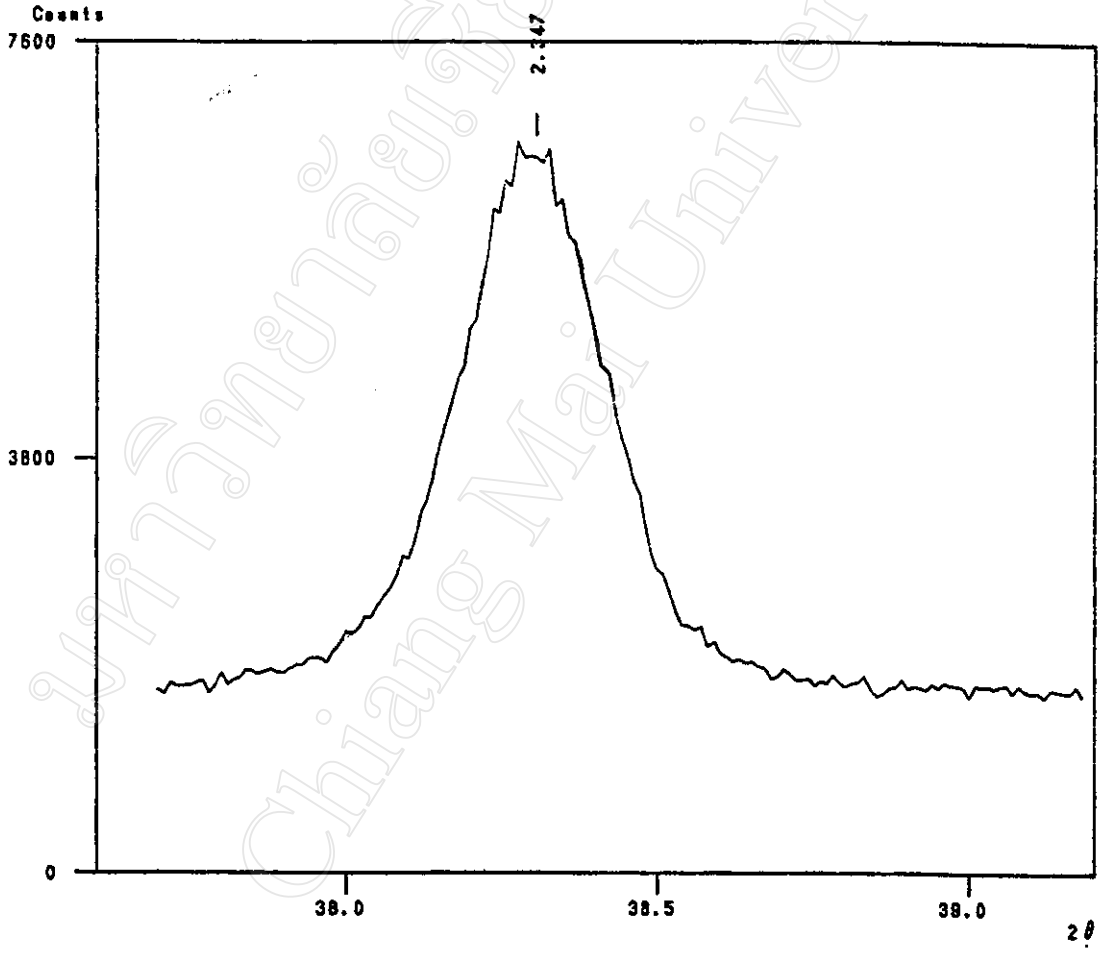

APPENDIX C

C.1 The Effect of Centrifuging.

When the tube rotate with angular velocity ω in the centrifuge, the centrifugal force, $F = m\omega^2 r$, will acts on PZT particles. The PZT particles in the tube were pressed by the force. This causes the density of the composites at the bottom larger than that at the top. The result is shown in the Figure A-C1. The samples were cut

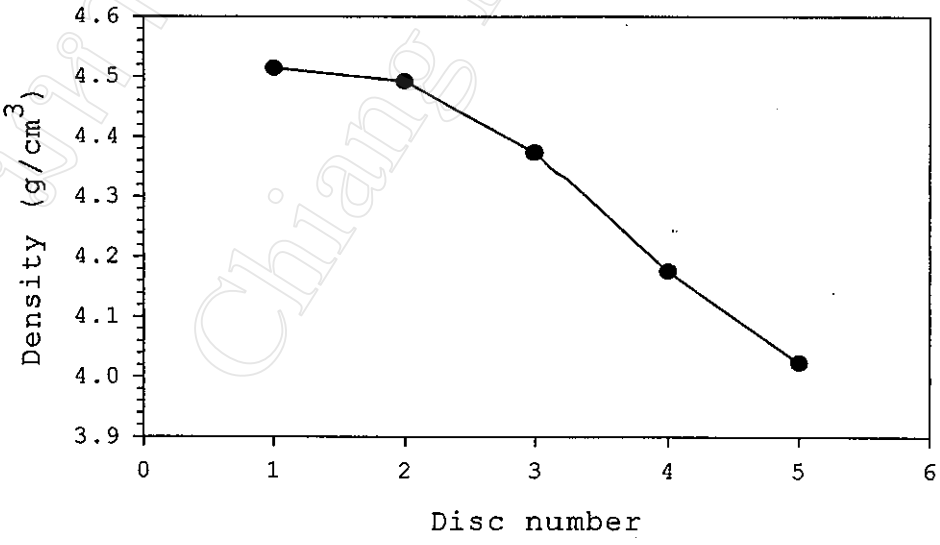

Fig. A-C1 Particle density VS dics number under the presence of the centrifugal force.

into disc shape starting from the first disc located at the bottom of the tube. The density of these samples was measured. The plot of the density as a function of disc number shows that the density was decreased with increasing of the disc number.

C.2 A Plot of d_{33} as A Function of Volume Percentage of Ceramics.

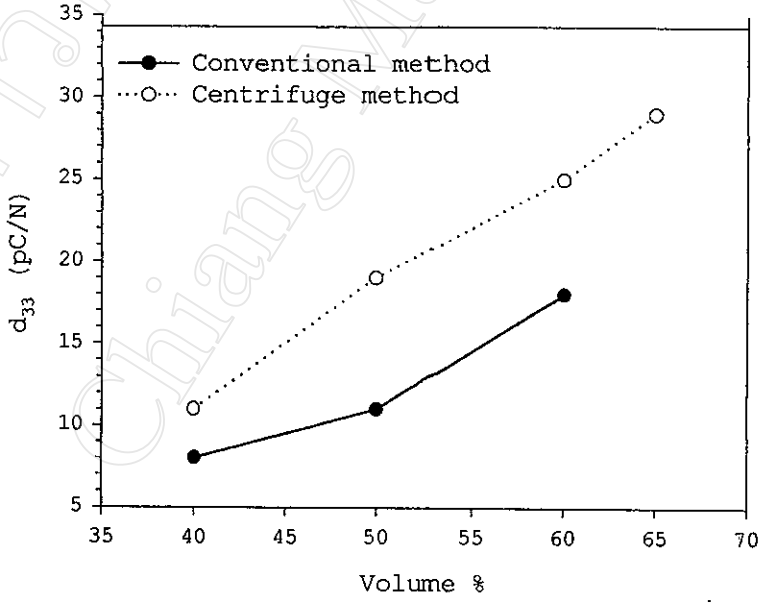

Fig A-C2 The d_{33} as a function of volume percentage of ceramics.

VITA

Name-Surname : Wim Nhuapeng

Date of Birth : 14 November 1964

Province : Nakhonpathom

Education : B.S.(Physics), Chiang Mai University, Chiang Mai, Thailand (1987).
M.S.(Physics), Chiang Mai University, Chiang Mai, Thailand (1989).

Scholarship : Ph.D. scholarship from the National Metal and Materials Technology Center of Thailand, June 1,1996-May 31,2000.

Publications :

1."Structure and Electrical Properties of RF-Sputtering Deposited Thin Ferroelectric $Pb(Zr_{0.52}Ti_{0.48})O_3$ Films", *J. Mater. Sci. Lett.*, **19**, 1913-1916, (2000) with T. Tunkasiri, Ye Qin and W. Thamjaree.

2."Analysis of X-Ray Diffraction Line Profiles of Lead Zirconate Titanate Using the Fourier Method", *In First National Symposium on Graduate Research*, Chiang Mai University, 10-11 June 2000, with T. Tunkasiri.

3."Microstructure and Mechanical Properties of 0-3 Piezoceramic/Polymer composites", *In Proceedings on Electron Microscopy, J.E.M.S.T.*, **15**[1], 99-100, (2001) with J. Tontrakoon and T. Tunkasiri.

4."Properties of 0-3 Lead Zirconate Titanate-Polymer composites Prepared in a Centrifuge", *J. Am. Ceram. Soc.*, **85**[3], (2002) with T. Tunkasiri.

JOURNAL OF MATERIALS SCIENCE LETTERS 19, 2000, 1913–1916

Structure and electrical properties of RF-sputtering deposited thin ferroelectric $Pb(Zr_{0.52}Ti_{0.48})O_3$ films

T. TUNKASIRI
Department of Physics, Faculty of Science, Chiang Mai University, Chiang Mai 50200, Thailand

YE QIN
Department of Physics, Jinan University, Guangzhou, 510632 People's Republic of China

W. NHUAPENG, W. THAMJAREE
Department of Physics, Faculty of Science, Chiang Mai University, Chiang Mai 50200, Thailand

Thin films of lead zirconate titanate ($Pb(Zr,Ti)O_3$ or PZT) have been extensively studied due to their applications in ferroelectric and piezoelectric devices. Some of the interesting applications are integrated non-volatile ferroelectric memories, surface acoustic wave devices, electro-optics, and piezoelectric transducers [1–3]. Many studies have been carried out to produce thin PZT films using radio frequency (rf) sputtering techniques [1, 4, 5]. Various ratios of Zr/Ti were employed as the target to produce the films, for example, 58/42 and 45/55 [1], 48/52 and 40/60 [2], 65/35 [4] and 55/45 [5]. Different ratios of Pb : Zr : Ti result in structural change with composition at constant temperatures in a solid solution range. For example, at about 350 °C, the $Pb(Zr_xTi_{1-x})O_3$ system has a tetragonal unit cell if $x < 0.5$, while it becomes a cubic unit cell when $x > 0.5$. The planar coupling coefficient and the relative permittivity show especially high values when $x = 0.52$ [6]. Therefore, it is interesting to attempt to obtain the thin film with the high permittivity at exactly $x = 0.52$ using various appropriate techniques. This paper presents our work on producing such a kind of PZT film using rf-sputtering deposition and studying the structure and electrical properties of the films.

Stoichiometric $Pb(Zr_{0.52}Ti_{0.48})O_3$ powder was used as the target. The powder was prepared from aqueous solutions of lead nitrate ($Pb(NO_3)_2$), zirconyl nitrate hydrate ($Zr(NO_3)_4 \cdot nH_2O$) and tetraisopropyl orthotitanate ($C_{12}H_{28}O_4Ti$) with the mole ratio of 1 : 0.52 : 0.48 respectively, following the method described by Tunkasiri [7]. The precipitate powder was filtered, dried and calcined at 800 °C prior to sputtering. Platinum sheet was used as the substrate. Two temperatures, 30 °C (room temperature) and 250 °C of the platinum substrates were used. The temperature control was carried out using a chromel-alumel thermocouple. The sputtering conditions adopted in the experiment are summarized in Table I.

All the as-sputtered PZT films were annealed (in air) at successive temperatures of 350 °C, 450 °C, 550 °C and 650 °C for 1 h at each step. X-ray diffractometry (XRD) and Auger electron spectroscopy (AES) were employed to analyze the phase transformation and the composition of the samples. The lattice parameter ratios (c/a) of the PZT films and calcined powder were calculated according to Cohen's methods [8].

A surface microstructural study of the films was carried out using a scanning electron microscope (SEM). Electrical measurements for the dielectric constant ε_r and the loss angle, tan δ were carried out in a metal-film-metal system, i.e. Pt-PZT-Al, which was formed by vacuum evaporating an aluminum electrode (0.8 mm. in diameter) on the top of the PZT film. The ferroelectric behavior of the films was characterized from P-E hysteresis loop measurements at 4 kHz following the method described by Sawyer and Tower [9].

A typical Auger spectrum is shown in Fig. 1. The Auger electron spectra of the PZT films (~1 μm) deposited at room temperature and/or hot (250 °C) substrates show no substantial differences (data not shown). However, the film deposited on the hot substrate exhibits more pronounced peaks of lead (Pb), zirconium (Zr) and titanium (Ti), as shown in Fig. 1. The film composition was determined based on the method of Chikaramane *et al.* [4] and the handbook of chemistry and physics [10]. The Auger electron spectrum clearly shows the Pb line at 93.2 eV, Zr lines at 120 eV and 147 eV, Ti lines at 384 eV and 417 eV, and O line at 516 eV. These results are close to that of Chikaramane [4] though a few peaks slightly shift. This may be due to discrepancies of the measurement. Some of X-ray diffractograms showing structure changes after annealing are shown in Fig. 2. It is found that the amorphous as-deposited film first transformed into a pyrochlore phase at 450 °C. On further annealing, the film crystallized into a ferroelectric phase of composition $Pb(Zr_{0.52}Ti_{0.48})O_3$ at 550 °C. The perovskite

TABLE I Sputtering deposition conditions

Target material	$Pb(Zr_{0.52}Ti_{0.48})O_3$ powder
RF power	200 W
Substrates	Pt sheet
Sputtering gas	Ar (100%)
Gas pressure	20–30 Pa
Distance between target and substrate	35 mm.
Deposition rate	2–3 nm/min
Film thickness	~1 μm
Temperature of substrate	Room temperature (~30 °C) and ~250 °C

0261–8028

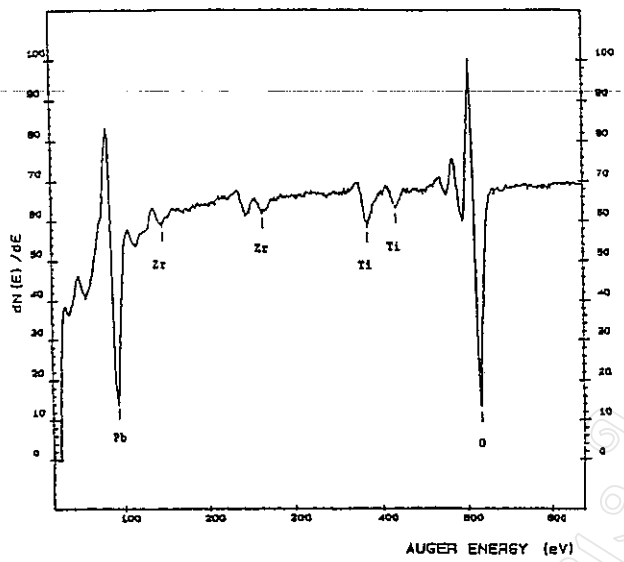

Figure 1 The Auger spectrum of the film sputter-deposited on the hot platinum sheet (250 °C), annealed at 650 °C, showing the Pb, Zr, Ti and O peaks. The compositional analysis is obtained from the measured peak to peak heights for the elements in the spectrum and weighting factors [4].

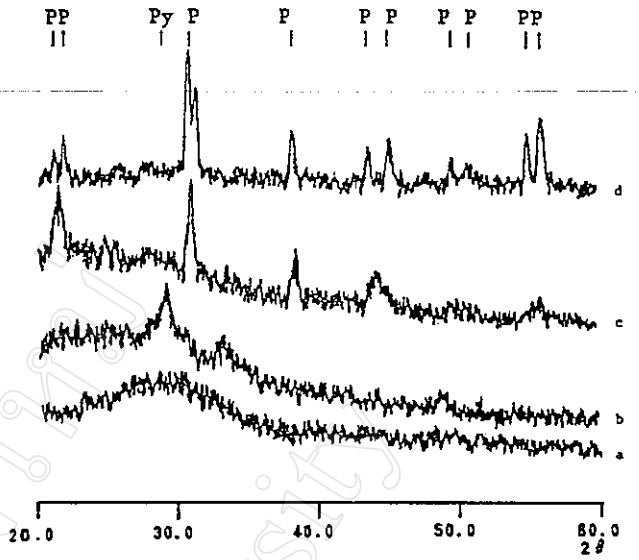

Figure 2 Phase evolution as a function of annealing temperature of the film deposited on the hot substrate. (a) as-deposited; (b) annealed at 450 °C; (c) annealed at 550 °C; (d) annealed at 650 °C.

tetragonal PZT was well pronounced at 650 °C. Indexing was carried out according to the recommendation from the Joint Committee on Powder Diffraction Standard (JCPDS) [11]. No other phase or impurity was detected by this method. The tetragonalities (ratios of c/a) of this film and calcined powder were calculated, to be 1.031 and 1.041 respectively. These are comparable to those obtained from Yi *et al.* [2] (as shown in Table II.). The amorphous as-sputtered film deposited on the substrate at room temperature however, showed pyrochlore and perovskite phases at 550 and 650 °C respectively. The results are summarized in Table II, together with those from the others [1, 2, 4, 12]. The ratio of c/a obtained from this film (post annealing at 650 °C) was 1.02.

Fig. 3 shows the P-E hysteresis loops of the PZT films after annealing at 650 °C. All samples exhibited good ferroelectric behavior. It is indicated from the shapes of the hysteresis loops that the ferroelectric property of

TABLE II PZT film phase evolution as a function of annealing temperature from this work and those of others

Sample	Substrate temperature (°C)	Phase evolution	Zr/Ti	c/a
This work	Room temperature	Amorphous as-deposited film transformed into pyrochlore and perovskite structure at 550 °C and 650 °C respectively.	52/48	1.02
	250	Amorphous as-deposited film transformed into pyrochlore phase at 450. Perovskite structure began to show at 550 °C and well pronounced at 650 °C.	52/48	1.03
Sreenivas *et al.* [1]	200	Rhombohedral and tetragonal structures showed after annealing at 550 °C and 750 °C respectively.	58/42	—
Yi *et al.* [2]	*	Tetragonal was found after firing at 760 °C	48/52 to 40/60	1.03 1.04
Chikaramane *et al.* [4]	200	Pyrochlore phase transformed into perovskite phase after annealing above 600 °C. Lead oxide was present.	65/35	—
Al-Shareef *et al.* [12]	*	Amorphous as-deposited films crystallized into pyrochlore phase at 500 °C. Perovskite structure showed up after annealing at 600 °C	53/47	—

*Preparation was carried out by sol-gel techniques.

TABLE III Comparison of the remanent polarization (Pr) and the coercive field (Er) values obtained in this work with those of others

Sample	Substrate temperature (°C)	Pr (μC/cm^2)	Ec (kV/cm)	Zr/Ti	ε_r	tan δ
This work	Room temperature	13.5	50	52/48	700	0.06
	250	17	55	52/48	750	0.06
Sreenivas *et al.* [1]	627	30	30	58/42	800	—
Yi *et al.* [2]	*	80	60	ranging from 40/60 to 60/40	~260	0.01
Chikaramane *et al.* [4]	200	25.6	17.1	55/45	—	—
Al-Shareef *et al.* [12]	*	14	35	53/47	—	—
Tu and Milne [13]	*	22–27	40–45	53/47	800–1000	~0.03

*Preparation was carried out by sol-gel techniques.

the film on the 30 °C - substrate is a little softer than that of the hot substrate.

The remanent polarization (Pr) and coercive field (Ec) values of the samples are shown in Table III. Comparison was made with those of others [1, 2, 4, 12, 13]. The dielectric constant (ε_r) and loss angle (tan δ) of the samples are also tabulated. The values of ε_r and tan δ obtained in this work are comparable to those of Tu and Milne [13], Sreenivas *et al.* [1] and Yi *et al.* [2] though our ε_r is bigger than that of Yi *et al.* [2] (Table III). However, Yi *et al.* [2] and Tu and Milne [13] used the sol-gel techniques to prepare their samples.

The scanning electron micrographs of the PZT films (Fig. 4) show that the films appearing to be crack free and well adhered to the substrates. The sample annealed at 650 °C yielded a denser film with a larger grain size (about 0.7 μm) than that annealed at 550 °C (about 0.5 μm). The grain sizes were determined by the line intercept method [14]. Both micrographs show an agglomeration of grains.

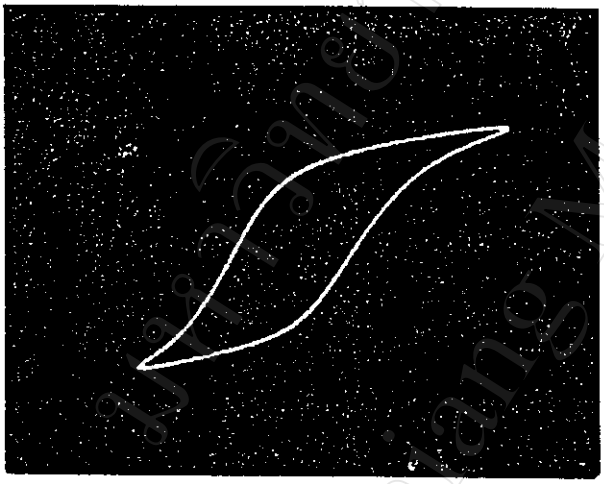

(a)

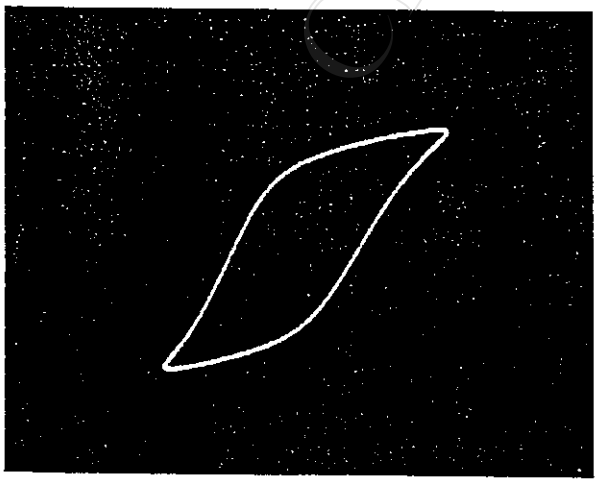

(b)

Figure 3 The P-E hysteresis loops of the PZT thin films after annealing at 650 °C. The substrate temperatures during sputtering are: (a) room temperature (30 °C); (b) 250 °C.

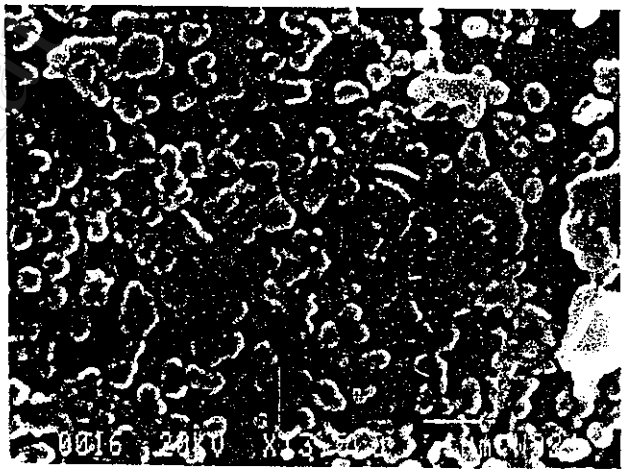

(a)

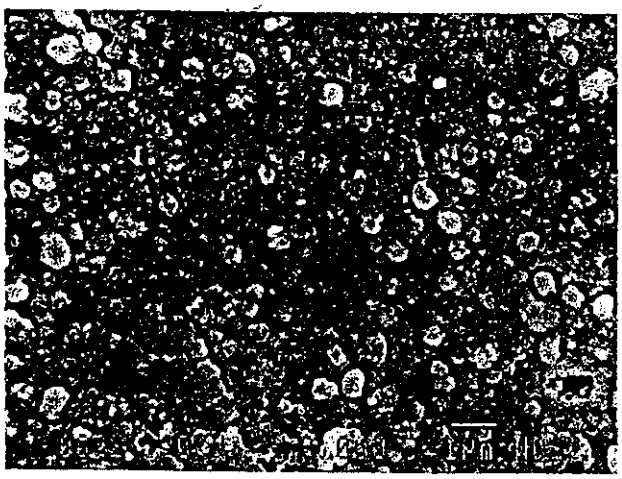

(b)

Figure 4 SEM micrographs of the PZT thin films deposited on the hot platinum substrates, after annealing at: (a) 550 °C; (b) 650 °C.

In conclusion, ferroelectric PZT thin films with the composition of $Pb(Zr_{0.52}Ti_{0.48})O_3$ about 1 μm thick have been prepared by rf-sputtering deposition on platinum substrates at 30 °C and 250 °C. For the 250 °C-substrate, deposition annealing resulted in transformation of the film phase from the initial amorphous to pyrochlore at 450 °C, crystallization above 550 °C and well pronounced perovskite tetragonal phase at 650 °C. The films formed are super-clean and have large grains. The remanent polarization (Pr), the coercive field (Ec), the dielectric constants and the loss angle of the films were comparable to those obtained from others. The results of this experiment confirm that the $Pb(Zr_{0.52}Ti_{0.48})O_3$ films have promising properties, pointing the way to further developments for capacitor applications.

Acknowledgments

The authors would like to express their sincere thanks to the National Metal and Materials Technology Center of Thailand which funded this project. We wish to thank Dr. L. D. Yu for his critical reading of the manuscript and useful comments and suggestions.

References

1. K. SREENIVAS, M. SAYER, D. J. BAAR and M. NISHIOKA, *Appl. Phys. Lett.* **52** (1988) 709.
2. G. YI, Z. WU and M. SAYER, *J. Appl. Phys.* **64** (1988) 2717.
3. Z. SUROWIAK, M. LOPOSZKO, I. N. ZAKHARCHENKO, A. A. BAKIROV, E. A. MARCHENKO, E. U. SVIRIDOV, V. M. MUKHORTOV and U. P. DUDKEVICH, *Thin Solid Films* **205** (1991) 76.
4. V. CHIKARAMANE, J. KIM, C. SUDHAMA, J. LEE and A. TASCH, *J. Elect. Mater.* **21** (1992) 503.
5. X. LI, J. LIU, Y. ZENG and J. LIANG, *Appl. Phys. Lett.* **63** (1993) 2345.
6. A. J. MOULSON and J. M. HERBERT, "Electroceramics Materials, Properties and Applications" (Chapman and Hall, London, 1990) p. 277.
7. T. TUNKASIRI, *Smart Mater. Struct.* **3** (1994) 243.
8. B. D. CULLITY, "Element of X-ray Diffraction" (Addison-Wesley, Reading, 1978) p. 363.
9. C. B. SAWYER and C. H. TOWER, *Phys. Rev.* **35** (1930) 269.
10. D. R. LIDE, "CRC Handbook of Chemistry and Physics," 73th ed. (CRC Press, 1992) p. 10.
11. Powder diffraction File, Joint Committee on Powder Diffraction Standards, (International Centre for Diffraction Data, Swarthmore, P.A., 1987) Card No. 33-784.
12. H. N. AL-SHAREEF, K. R. BELLUR, O. AUCIELLO and A. I. KINGON, *Thin Solid Films* **256** (1995) 73.
13. Y. L. TU and S. J. MILNE, *J. Mater. Sci.* **30** (1995) 2507.
14. Annual Book of ASTM Standards, Designation E: 112-82 Easton, MD., 1992.

Received 4 February
and accepted 24 March 2000

Analysis of X-Ray Diffraction Line Profiles of Lead Zirconate Titanate Using the Fourier Method

W. Nhuapeng T. Tunkasiri

Department of Physics, Faculty of Science, Chiangmai University, 50200

ABSTRACT

Lead Zirconate Titanate (PZT) powder was prepared by solid state reaction.The x-ray line broadening produced in PZT powder was analyzed by Fourier method to estimate the particle size and microstrain. It was found that as the annealing temperature is increased, the microstrain was found to decrease accorded by an increase in particle size. Scherrer formula was also used to calculate the particle which yielded a smaller particle size.

CODE: ST-61

J.E.M.S.T. Vol.15 No.1, pp.99-100, 2001
Printed in Thailand

W. Nhuapeng
J. Tontrakoon
T. Tunkasiri

Microstructure and Mechanical Properties of 0-3 Piezoceramic/Polymer Composites

Department of Physics, Faculty of Science, Chiang Mai University,
Chiang Mai 50200, Thailand

Composites consisting of piezoelectric and polymers have been found to combine the desired piezoelectric sensitivity and dielectric constant of Ceramic with the low density and flexibility of polymer.[1] Therefore, piezoelectric/polymer composites are intended for underwater hydrophone and biomedical applications.[2] Because it has appropriate acoustic coupling coefficient, matching between water and tissue.[3] The 0-3 connectivity is one of the types that the arrangement of component phases in the composites not so complicated to prepare. In this work, 0-3 piezoelectric ceramic/polymer composites were prepared by centrifuge technique. Lead zirconate titanate (PZT) and polyester resin were employed as piezoelectric ceramic phase and polymer or matrix phase respectively. The percentage by volume of PZT was varied and centrifuged in polyester resin with speed of 4500 cycles per minute. Spinning time was 30 minutes. By this technique the volumetric fraction of PZT up to 65 percent. After allowing the composites to settle the sample rods of about 1 cm. in diameter were cut into disc shape with the thickness of 1.0 mm. Density and microstructure of composites were studied by Archimedes method and Scanning Electron Microscope (SEM) respectively. Besides, the acoustic impedance of composites was investigated by echo-shift method.[4] Scanning electron micrographs show the distribution of PZT powder in polyester resin. Small particle size was found to pack together closer and denser than that of the large particle size (Fig. 1(a-d)). We also found that if the volumetric percentage of PZT increases, density and acoustic impedance of composites tend to increase as shown in Table 1.

Table 1 Density and acoustic impedance of the composites with various ceramic loading.

Ceramic loading (Vol%)	Density (g/cm^3)	Acoustic impedance
Polyester resin	1.17	2.51
40	3.60	6.90
50	4.29	9.59
60	4.85	11.47
65	5.21	12.04
PZT ceramic disc	7.78	28.29

Acknowledgement

The authors would like to express their sincere thanks to the Nation Science and Technology Development Agency for funding this work.

References

1. Janas, V.F. and A. Safari (1995) Overview of Fine-Scale Piezoelectric Ceramic/Polymer Composite Processing, *J. Am. Ceram. Soc.*; **78**: 2945-2955.
2. Smith, W.A. (1989) The Pole of Piezocomposites in Ultrasonic Transducer, *Ultrasonic Symposium*: 755-766.
3. Safari, A. (1994) Development of Piezoelectric Composites for Transducer, *J. Phys. III France*; **4**: 1129-1149.
4. Bui, T. and W. Unsworth (1988) Specific Acoustic Impedances of Piezoelectric Ceramic and Polymer Composites Used in Medical Applications, *J. Acoustl Soc. Am.*, **83**: 2416-2421.

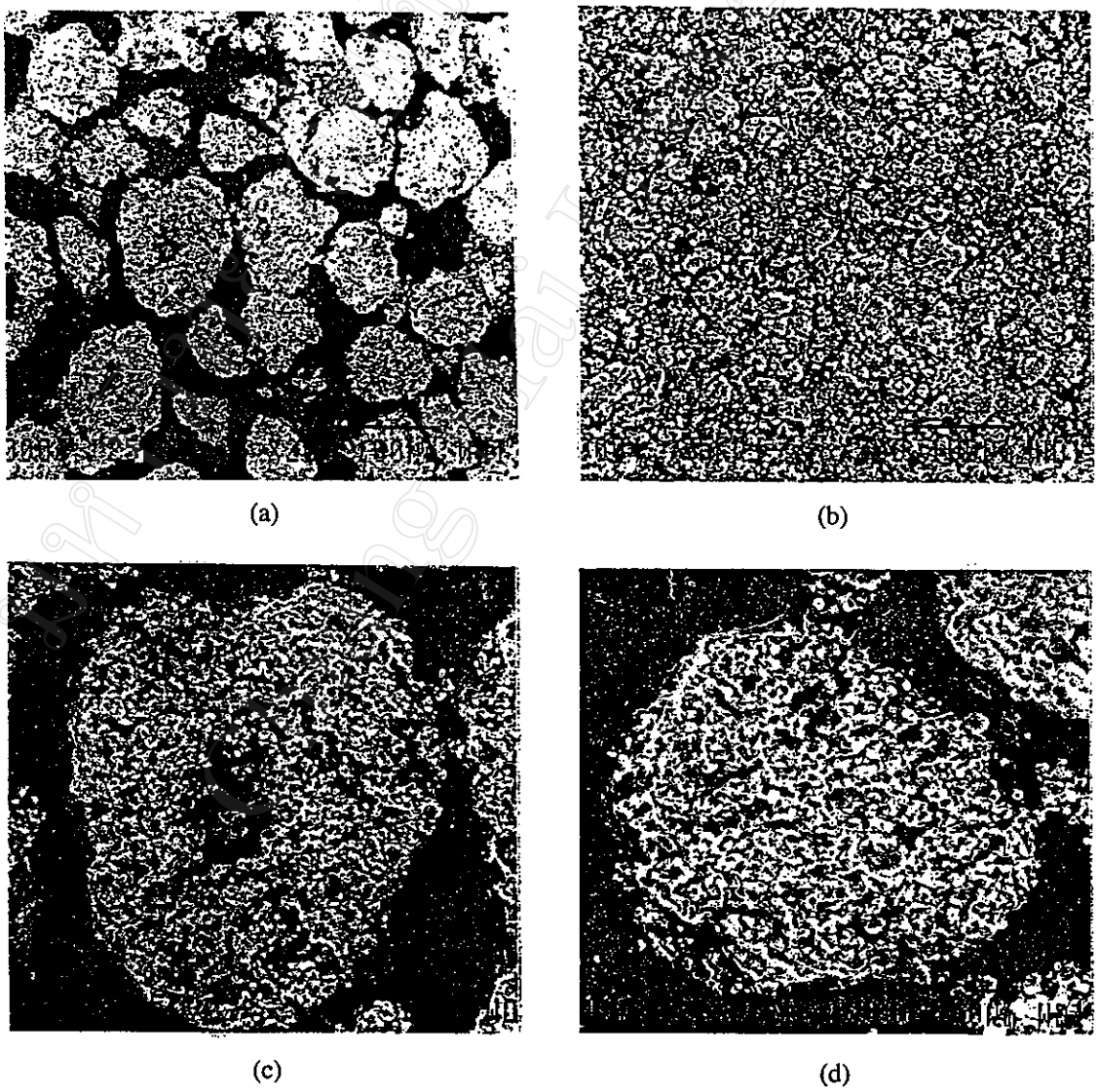

Figure 1. Distribution of the PZT powder in the polyester resin (a) particle size 150 μm with volumetric fraction 60% (b) particle size 65 μm with volumetric fraction 65%, (c) and (d) particle of PZT powder of (a) and (b) respectively.

The American Ceramic Society

Authors
Dr. Tawee Tunkasiri
Mr. W. Nhuapeng

10/29/2001

Dr. Tawee Tunkasiri
Chiang Mai University
Faculty of Science
Dept. of Physics
Chiang Mai 50200
Thailand

Dear Dr. Tunkasiri:

The paper entitled "Properties of 0-3 Lead Zirconate Titanate - Polymer Composites Prepared in a Centrifuge" (Manuscript #187829) has been accepted for publication in the Journal. Our editorial staff will be reviewing the paper and may need to request minor editorial changes. You will receive page proofs for final checking before your paper is published.

If you have not previously sent us a signed page charge form, please note the enclosed form and memorandum outlining the Society's policy concerning page charges.

We are looking forward to your continued cooperation in getting this work into print.

Sincerely,

Dr. Harlan Anderson
harlanua@umr.edu
Journal Editor

[illegible] Box 6136
[illegible] Ohio 43086-6136
[illegible] 614/890-4700
[illegible] 6109
[illegible] acers.org
[illegible] acers.org

journal

J. Am. Ceram. Soc., 85 [3] 000–000 (2002)

Properties of 0-3 Lead Zirconate Titanate–Polymer Composites Prepared in a Centrifuge

W. Nhuapeng and Tawee Tunkasiri*

Department of Physics, Faculty of Science, Chiangmai University, Chiangmai 50200, Thailand

The purpose of this work was to present the electrical and piezoelectric properties of the 0-3 piezoceramic–polymer composites prepared by spinning the lead zirconate titanate (PZT) powders with polyester resin in a centrifuge. PZT powders with average sizes of 55 and 160 μm were used and mixed in the resin with different volumetric percentages. The dielectric and piezoelectric properties such as permittivity, loss angle, electromechanical coupling factor, and piezoelectric coefficient were measured. The mechanical quality factor was calculated. The acoustic impedance was accessed by the echo-shift method. The results were analyzed and fit to mechanical models. Distribution of the ceramic particles in the polyester-resin phase was examined by scanning electron microscopy. Smaller-ceramic-particle composites seemed to form denser samples. Most of the properties showed linearly varying as the volumetric percentage of the ceramic phase. The fabrication using the centrifuging techniques resulted in more homogeneity of the ceramic and polymer phases, and the fabricated samples could be loaded up to 65% or more with the ceramic powders.

I. Introduction

MANY types of transducers of piezoceramic–polymer composites have been widely used in several applications, such as hydrophones and biomedical transducers. This is because of their properties, which indicate advantages over single-phase ceramics. Early reports concerning the properties of single-phase ceramics, mainly lead zirconate titanate (PZT), reveal that they exhibit high dielectric constant (ε_r) and density (ρ), when compared with those of the composites. These properties of the ceramics lead to high acoustic impedance (Z) and to difficulty in matching to water and human tissue.[1] Besides, they are brittle, probably not flexible enough to suit a curved surface. On the contrary, the piezoceramic–polymer composites exhibit a relatively low ρ, thus low Z and high flexibility. Therefore, they are appropriate candidates to be conformed and molded to any designed surface. Among these composites, the connectivity of the 0-3 piezoceramic polymer is considered to be rather uncomplicated, and the material can be prepared in various forms making it comparatively easy to be mass produced. In this type of composite, the ceramic powder has no physical particle–particle contact, while the polymer phase has a three-dimensional connection.[2] There are many methods to prepare this composite. The conventional calendering method is relative simple. The piezoceramic can be loaded <50% by volume.[3] As the properties of the composite such as the piezoelectric constant (d_{33}) and the electromechanical coupling factor (k_t) vary as the percentage of the piezoceramic volume, attempts to load the piezoceramic >60% have been conducted. However, they are restricted by the methods of mixing. Many techniques were studied regarding this aspect such as tape casting[3] (60%), painting[4] (70%), and colloidal[5] (70%), although their processes are still complicated. The present work is to investigate the fabrication and properties of the 0-3 piezoceramic–polymer composite prepared by the centrifuge method to spin the piezoceramic particles into the polymer as much as possible by the centrifugal force. With this method, we expect to load piezoceramic <60% by volume or slightly higher, since too much of the ceramic phase could reduce its flexibility. The piezoelectric properties (d_{33} and k_t), the mechanical properties (ρ and Z), and the microstructure of the composites have been characterized.

II. Experimental Procedure

According to Safari,[2] the bigger particle size PZT powder in the 0-3 composites had the tendency of yielding a higher value of d_{33}. To obtain the 0-3 composites with considerable big PZT particles, commercial PZT powder (Product 40/30, Advanced Ceramic Limited) was atmospherically sintered at 1200°C into samples, which were then pulverized and sieved through nylon mesh (No. 100). The distribution of the particle size of the sieved particles was assessed using a sedimentograph (Model Analysette 22, Shimadzu Corp., Tokyo, Japan). The average value of the particle size was ~160 μm. The powders were then mixed into polyester resin with varied ratios of 40%, 50%, 60%, and 65% by volume. However, 65% of PZT powder could not be loaded into resin, probably because of the large particle size, which might cause some packing problem. Therefore the powders again were sieved (No. 300). The average value of the particle size was ~55 μm. The sieved powders were then mixed into polyester resin with the volumetric ratio of 65%. Approximately 2 cm^3 of each of the samples which were slurry at the moment, were put into plastic tubes of ~1 cm in diameter. They were spun in a centrifuge. After spinning with 4500 rpm for 30 min, the samples were allowed to settle for a few minutes. The composites (in the plastic tubes) were cut into disks with a thickness of 1 mm.

The samples were polished after the plastic shells were removed. The density of the composites was measured. Before determination of the dielectric and piezoelectric properties of the composites, the samples were electroded by applying a silver paste (Product Electrodrag 1415M, Acheson) to the top and bottom surfaces. Poling was conducted in silicone oil at 80°C with a poling field of 10 kV/mm for 20 min. The ε_r, the loss factor (tan δ), and the coupling factor (k_t) were measured using an LCZ meter (Model 4276, Hewlett–Packard, Palo Alto, CA). The piezoelectric coefficient (d_{33}) was measured using a piezo-d_{33}-meter (Model CADT, Berlincourt). The PZT-particle distribution was accessed by a scanning electron microscope (SEM). All ceramics were investigated by X-ray diffraction (XRD). Indexing was conducted according to the recommendation from the Joint Committee on

A. Safari—contributing editor

Manuscript No. 187829. Received March 26, 2001; approved October 16, 2001.
Supported by the National Metal and Materials Technology Center of Thailand.
*Member, American Ceramic Society.

Table I. Showing Electrical Properties of Composite

Samples	Volume (%)	Average particle size (μm)	ε_r (1 kHz)	tan δ (1 kHz)	d_{33} (pC/N)
PZT + Polyester resin	40	160	45	0.0140	10
	50	160	52	0.0138	18
	60	160	84	0.0141	26
	65	55	88	0.0353	29
PZT + PVC thin film[3]	60	2.3	134	0.23	29
PZT + Polyurethane[4]	60	1–2	51 ± 5	0.02	25 ± 5
	70	1–2	45 ± 5	0.04	28 ± 5
PZT + PVDF[7]	65	2	45		33

Powder Diffraction Standards (JCPDS; now International Centre for Diffraction Data (ICDD)).[6]

III. Results and Discussion

The XRD result of each sample shows that all the diffraction profiles are attributed to PZT. No other phase or impurity is detected. The fabrication of the 0-3 composites by spinning in a centrifuge possibly leads to a high volumetric percentage of the ceramic phase (>65%). Smaller particles of PZT seem to yield a higher volumetric percentage of ceramic in the composites. The electrical and piezoelectric values are presented in Table I with those of Fries and Moulson,[3] Hanner *et al.*,[4] and Cai *et al.*[7] The ε_r, tan δ, and d_{33} are larger in the higher percentage of the ceramic phase. All the d_{33} values obtained are comparable to those of Fries and Moulson,[3] Hanner *et al.*,[4] and Cai *et al.*,[7] who used different preparation methods, such as calendering, painting, and hot roller, respectively. However, the ε_r and tan δ values which have been obtained from our work (at 60%) are less than that of Fries and Moulson.[3] This may be because the composites produced by Fries and Moulson employed platelets PZT as filler, in which part of the composite structure was pseudo 1–3. In our case, the d_{33} values are in the range of 10 and 29 pC/N, which are less than those reported by Safari (45 pC/N).[2] This may be because the different methods of poling since Safari used the corona method.

Table II. Showing k_t and Q_m Values

Sample	Volume (%)	K_t	Q_m
This work	40	0.33	4.43
	50	0.45	5.74
	60	0.37	9.20
	65	0.41	9.97
Han *et al.*[5]	70	0.17	5–8
Wersing[9]	70	0.50	15
Slayton and Setty[10]	70	0.61	9.1

The k_t and mechanical-quality factor (Q_m) were calculated using the formulae suggested by Moulson and Herbert.[8] These are

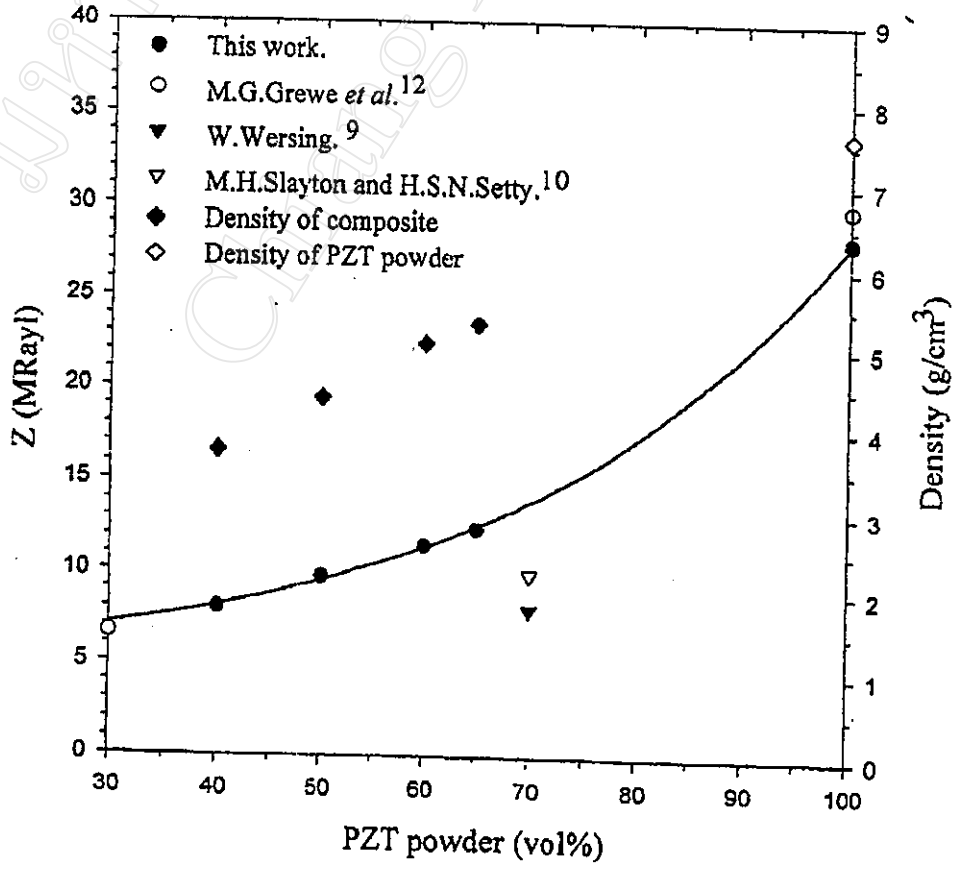

Fig. 1. Acoustic impedance (Z) and density (ρ) plotted against volume percentage of PZT powder.

tabulated in Table II with that of others.[5,9,10] The values of k_t and Q_m obtained in our work were in the range of 0.33–0.45 and 4.4–9.9, respectively, which were comparable to those reported by Han *et al.*,[5] Wersing,[9] and Slayton and Setty.[10] Although their composites were prepared from colloidal PZT and epoxy, ceramic and plastic, and single-particle-layer piezoelectric PZT and epoxy, respectively.

The Z value of the composites was measured using the method of echo-shift suggested by Bui *et al.*[11] The Z value and the density of the composites are shown in Fig. 1, together with those of Wersing,[9] Slayton and Setty,[10] and Grewe *et al.*[12] The ρ and Z values varied as the ceramic percentage in the composites. The Z values were in the range of 7.43–9.97 MRayls for the ceramic percentages of 40%–65%, respectively. The results were comparable to those reported by Wersing,[9] Slayton and Setty,[10] and Grewe *et al.*[12] The Z data were analyzed to fit with the Voigt, Reuss, and logarithmic models according Grewe *et al.*[12] It was found that the data most likely fit with the logarithmic model.

Figure 2 shows SEM micrographs of the distribution of the PZT powder in the composites. The fabrication by the centrifuging method shows a considerably good distribution of the ceramic particles in the polymer phase. The smaller PZT powders (55 μm) seem to pack closer and denser than the larger PZT particles (160 μm). This agrees well with the ρ values (Fig. 1), which reveals that the composites with smaller PZT particles (~ 55 μm) at 65% possess higher density.

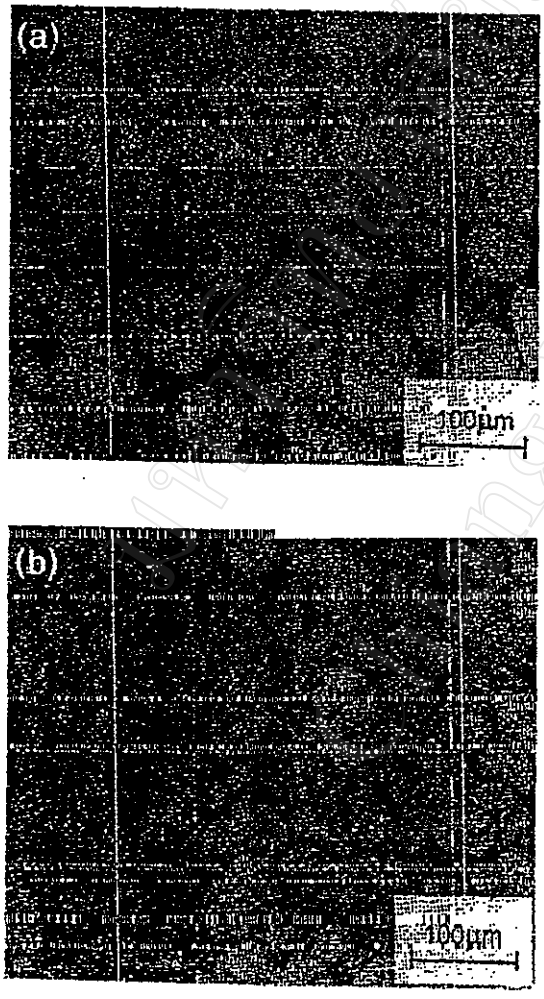

Fig. 2. SEM micrographs of the composite surfaces with various volume percentages of PZT powder: (a) 60% and (b) 65%

IV. Summary

Fabrication of 0-3 piezoceramic–polymer composites was conducted by spinning PZT powders and polyester resin in a centrifuge. The PZT powders, with an average size of 160 μm, were used as filler mixed into resin with varied ratios of 40%, 50%, 60%, and 65% by volume. The results indicated that 65% of 160 μm PZT powder could not be loaded into resin, probably because of the packing problem. Smaller powders (average size of 55 μm) were used at this volume content (65%). The physical properties, such as ε_r, tan δ, k_t, and d_{33}, increased with increased volumetric percentages. With smaller PZT powders, the mixtures were more homogeneous and denser; they also could be loaded up to 65% or more with ceramic powder. The Z value of the composites obtained, analyzed with three mechanical models, showed that the data most likely fit the logarithmic model.

Acknowledgments

The authors would like to thank Dr. L. D. Yu for his useful comments and correction on the manuscript.

References

[1]T. R. Gururaja, W. A. Schulze, L. E. Cross, R. E. Newnham, B. A. Auld, and Y. J. Wang, "Piezoelectric Composite Materials for Ultrasonic Transducer Application-Part 1," *IEEE Trans. Sonics Ultrason.*, SU-32, 489–97 (1985).

[2]A. Safari, "Development of Piezoelectric Composites for Transducers," *J. Phys. III*, 4, 1129–49 (1994).

[3]R. Eriet and A. J. Moulson, "Fabrication and Properties of an Anisotropic PZT/Polymer 0-3 Composite," *J. Mater. Sci.: Mater. Electron.*, 5, 238–43 (1994).

[4]K. A. Hanner, A. Safari, R. E. Newnham, and J. Ruud, "Thin Film 0-3 Polymer/Piezoelectric Ceramic Composites: Piezoelectric Paints," *Ferroelectrics*, 100, 255 (1989).

[5]K. H. Han, A. Safari, and R. E. Riman, "Colloid Processing for Improved [illegible] of Flexible 0-3 Ceramic Polymer Composites," *J. Am. Ceram. Soc.*, 74, 1669–702 (1991).

[6]Powder Diffraction File, No. 33-784, Joint Committee on Powder Diffraction Standards, Swarthmore, PA (now International Centre for Diffraction Data, Newtown Square, PA).

[7]X. Cai, C. Zhong, S. Zhang, and H. Wang, "A Surface Treating Method for Ceramic Particles to Improve the Compatibility with PVDF Polymer in 0-3 Piezoelectric Composites," *J. Mater. Sci. Lett.*, 16, 253–54 (1997).

[8]A. J. Moulson and J. M. Herbert, *Electroceramics*, 1st Ed.; pp. 274–76. Chapman and Hall, London, U.K., 1993.

[9]W. Wersing, "Composite Piezoelectrics for Ultrasonic Transducer"; pp. 212–3 in *IEEE International Symposium on Applied Ferroelectrics*. Institute for Electrical and Electronic Engineers, New York, 1986.

[10]M. H. Slayton and H. S. N. Setty, "Single Later Piezoelectric-Epoxy Composite"; pp. 90–92 in *IEEE International Symposium on Applied Ferroelectrics*. Institute for Electrical and Electronic Engineers, New York, 1990.

[11]I. Bui and H. L. W. C. J. Unsworth, "Specific Acoustic Impedances of Piezoelectric Ceramic and Polymer Composites Used in Medical Applications," *J. Acoust. Soc. Am.*, 83, 2416–21 (1988).

[12]M. G. Grewe, T. R. Gururaja, R. E. Newnham, and T. R. Shrout, "Acoustic Properties of Particle/Polymer Composites for Transducer Backing Applications"; pp. 716–19 in *IEEE Ultrasonic Symposium*. Institute for Electrical and Electronic Engineers, New York, 1989.

Keywords: lead zirconate titanate; polymers/polymerization; composites; processing